# STREAMLINE SIMULATION OF SURFACTANT ENHANCED

# AQUIFER REMEDIATION

A Thesis

by

DOUGLAS IRVIN TUNISON

Submitted to the Office of Graduate Studies of
Texas A&M University
in partial fulfillment of the requirements for the degree of
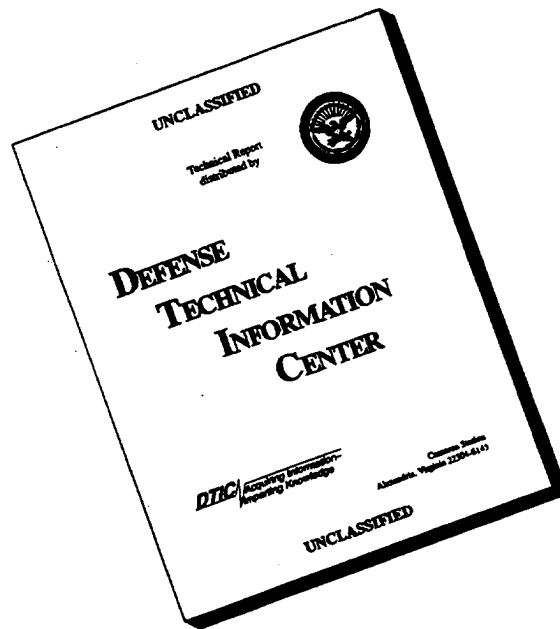
MASTER OF SCIENCE

December 1996

Major Subject: Petroleum Engineering

# DISCLAIMER NOTICE

UNCLASSIFIED

Technical Report
distributed by

**DEFENSE**
**TECHNICAL**
**INFORMATION**
**CENTER**

*DTIC* Acquiring Information
Imparting Knowledge

Cameron Station
Alexandria, Virginia 22304-6145

UNCLASSIFIED

## THIS DOCUMENT IS BEST QUALITY AVAILABLE. THE COPY FURNISHED TO DTIC CONTAINED A SIGNIFICANT NUMBER OF PAGES WHICH DO NOT REPRODUCE LEGIBLY.

| AD NUMBER | DATE<br>20 Aug 96 | DTIC ACCESSION<br>NOTICE |
|---|---|---|
| **1. REPORT IDENTIFYING INFORMATION**<br><br>**A. ORIGINATING AGENCY**<br>NAVAL POSTGRADUATE SCHOOL,MONTEREY,CA 93943<br>**B. REPORT TITLE AND/OR NUMBER**<br>Streamline Simulation of Surfactant Enhanced Aquifer Remediation<br>**C. MONITOR REPORT NUMBER** Texas A&M U.<br>TUNISON, Douglas I. Thesis December 1996<br>**D. PREPARED UNDER CONTRACT NUMBER**<br>N00123-89-G-0598<br><br>**2. DISTRIBUTION STATEMENT**<br><br>APPROVED FOR PUBLIC RELEASE;<br>DISTRIBUTION UNLIMITED | | <u>REQ</u><br><br>*1. Put<br>on r*<br>*2. Con*<br>*3. Atta<br>ma*<br>*4. Use<br>inf*<br>*5. Do r<br>for*<br><br><u>DTIC</u><br><br>*1. Ass*<br><br>*2. Ret*<br><br>19960904 046 |

DTIC Form 50
DEC 91                                    PREVIOUS EDITIONS ARE OBSOLETE

# STREAMLINE SIMULATION OF SURFACTANT ENHANCED

# AQUIFER REMEDIATION

A Thesis

by

DOUGLAS IRVIN TUNISON

Submitted to the Office of Graduate Studies of
Texas A&M University
in partial fulfillment of the requirements for the degree of

MASTER OF SCIENCE

December 1996

Major Subject: Petroleum Engineering

# STREAMLINE SIMULATION OF SURFACTANT ENHANCED
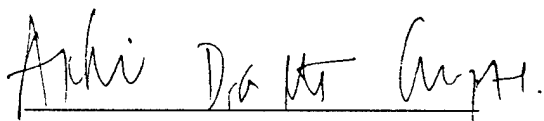
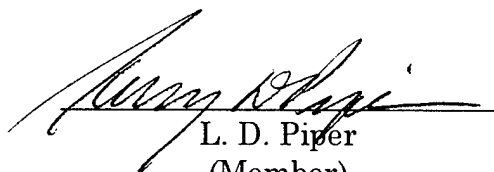# AQUIFER REMEDIATION

A Thesis

by

DOUGLAS IRVIN TUNISON

Submitted to Texas A&M University
in partial fulfillment of the requirements
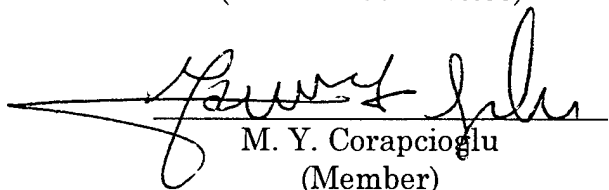for the degree of

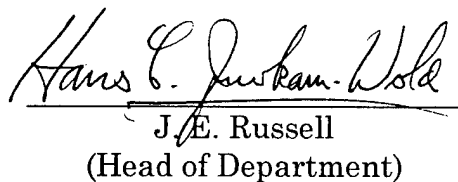MASTER OF SCIENCE

Approved as to style and content by:

_____
A. Datta-Gupta
(Chair of Committee)

_____
L. D. Piper
(Member)

_____
M. Y. Corapcioglu
(Member)

_____
J. E. Russell
(Head of Department)

December 1996

Major Subject: Petroleum Engineering

# ABSTRACT

Streamline Simulation of Surfactant Enhanced Aquifer Remediation.

(December 1996)

Douglas Irvin Tunison, B.S., University of Kansas

Chair of Advisory Committee: Dr. A. Datta-Gupta

Nonaqueous Phase Liquids (NAPLs) are a recognized source of groundwater contamination. Surfactant Enhanced Aquifer Remediation (SEAR) shows promise in increasing the efficiency and effectiveness over traditional "pump and treat" NAPL remediation processes. Laboratory results are not always consistent with the effects observed in field applications because of the complex interactions that occur in the subsurface. Mathematical modeling is required to enable accurate prediction and understanding of SEAR.

This study develops a SEAR computer simulator that is fast, robust, and accurate. The new code applies fractional flow theory in conjunction with streamline theory to predict residual saturation, saturation distribution, production rate and cumulative production histories. The model is three dimensional and capable of modeling heterogeneity anisotropy. The SEAR simulator models mobilization of residual NAPL

through the effects of surfactant on the relative permeability curves. The solubilization effects are modeled by constant partition coefficients. The SEAR simulator is compared to a state of the art, high resolution, finite difference simulator (UTCHEM) under a variety of conditions. The predictions of the new SEAR simulator show close agreement with those predicted by UTCHEM. The streamline simulator is orders of magnitude faster than UTCHEM and is ideally suited for screening studies.

# DEDICATION

To Lisa.

# ACKNOWLEDGMENTS

# TABLE OF CONTENTS

# LIST OF TABLES

# LIST OF FIGURES

# CHAPTER I

# INTRODUCTION

## Background

The prevalence of organic solvents and other nonaqueous phase liquids (NAPLs) in groundwater aquifers is recognized as an impediment to aquifer remediation. The requirement to clean up this contamination has led to wide spread study of NAPL transport and dissipation in porous media. The ability to locate and remediate NAPLs is still in the testing stage.

Residual saturation of NAPLs can range from 5% to 40% of the pore volume.[1,2] Because of the low solubility of NAPLs displaced by water, the residual organic phase can remain a long term source of contamination. Also, the low solubility and residual saturation of NAPL contaminants makes the traditional treatment method of flushing the aquifer with water (also known as "pump and treat") inefficient because it fails to mobilize the trapped NAPL. Surfactant technology is a promising proposed alternative treatment to conventional methods for the removal of trapped organic phase liquids.[3]

Surfactant enhanced remediation works in the following manner. A low

This thesis follows the style of the *Journal of Petroleum Technology.*

concentration aqueous phase surfactant solution is injected into a contaminated aquifer. Because the NAPL is partially soluble in both the oleic phase and the aqueous phase, the surfactant tends to increase the solubility of the organic phase in water. The surfactant also tends to lower the interfacial tension between the organic contaminant and water, thus mobilizing the NAPL and reducing the residual saturation of the trapped organic phase. The solubilized or mobilized organic phases are then flushed out using a chase fluid of water or brine.

Most research in surfactant flushing technology to date is focused primarily at its application to enhanced oil recovery. Much of the work in the mathematical modeling of surfactant enhanced aquifer remediation does not adequately represent the complex physical and chemical behavior that occurs in surfactant remediation.[4] There has been little study of surfactant treatment of NAPL contaminated sites in either the laboratory or the field. Although the laboratory results are very promising, the field studies show mixed results. This is likely because of the complex interactions that occur in the ground. There is a need to model this process mathematically so that field applications may be designed and so that the field data collected may be analyzed and understood.

## Objectives

The primary objective of this study is to develop a computer model to simulate surfactant enhanced remediation (SEAR) of nonaqueous phase liquids (NAPLs) commonly found as contaminants in groundwater aquifers. The model will be fast, stable, and, with simple enhancements, provide results that are acceptable for use in planning contaminant remediation on site using a desktop PC.

The model developed in this study uses a streamline aquifer simulator that is orders of magnitude faster than simulators that are based on a finite difference solution. Fractional flow theory is applied to incorporate the effects of surfactant on simultaneous immiscible two phase flow. This simplified modeling of the mobilization and solubilization of trapped NAPL by surfactants appears to capture physio-chemical aspects of SEAR with reasonable accuracy.

The performance of a proven SEAR simulator, UTCHEM developed at the University of Texas at Austin, is tested for sensitivities to a number of aquifer parameters. These results serve as a benchmark for judging the performance of the streamline model. The sensitivity studies are repeated with the newly developed streamline model and its performance compared to the benchmarks established by the finite difference SEAR simulator.

# CHAPTER II

# LITERATURE REVIEW

## Surfactants and Surfactant Enhanced Remediation

Beginning in the 1970's, research peaked in the use of surfactants to improve oil recovery. From this research, a large body of knowledge, both theoretical and practical, developed in the use of surfactants in subsurface environments. Similarities exist between enhanced oil recovery (EOR) and cleanup of subsurface contamination. The standard method of remediation using conventional pump and treat methods is not efficient or effective when dealing with strongly sorbed organics such as PCBs and PAHs or when an organic like PCE or TCE exists in a residual and thus, immobile phase.[5] Application of surfactant technologies to the cleanup of such contaminated groundwater aquifers is currently undergoing extensive investigation[6] and initial results are promising.[7]

In simple terms, a surfactant is a molecule that has both hydrophilic and lipophilic parts. This causes the surfactant molecules to accumulate at the interface between phases. Of special interest is the accumulation of the surfactant molecules at the NAPL-aqueous phase interface. The molecules tend to accumulate with their lipophilic tail in the NAPL phase and the

hydrophilic head in the aqueous phase. A characteristic that distinguishes surfactants from other amphiphilic molecules such as alcohol is their tendency to form aggregates of surfactant molecules after the concentration exceeds some critical value.[5,8] These aggregates are known as micelles. The micelles tend to form with the hydrophilic heads pointing outward and the lipophilic tails, inward. Consequently, the interior of the globule attracts NAPL molecules. This tendency to solubilize organic compounds is important to the efficiency of surfactant enhanced aquifer remediation and is discussed in more detail below. This characteristic results in the formation of small globules of dispersed organic droplets. These dispersed organic droplets are then flushed from the aquifer and can then be treated on the surface.

A second important effect of surfactants on organics is the mobilization of the trapped residual phases by the reduction in interfacial tension between the organic and aqueous phases.[9] Under normal circumstances, the viscous forces between the organic phase and the aqueous phase are much smaller than the capillary forces and the result is that 20% to 40% of the organic phase remains trapped during a normal waterflood operation. Usually, a reduction in interfacial tension (IFT) of three to four orders of magnitude is required to mobilize the trapped organic phase.[6] A small amount of surfactant will result in a large reduction in interfacial tension,

easily reducing the IFT below the point required for mobilization. The amount of surfactant required is limited primarily by the retention of the surfactant by the aquifer rock by adsorption. The volume of injected surfactant required is suggested to be about 20% greater than the surfactant adsorbed for enhanced oil recovery purposes.[10] Mobilization is reported to be a more efficient process of removing contaminants from aquifers than solubilization.[9] This observation is corroborated by the results of this study. Unfortunately, mobilization is not always desirable in aquifer remediation because the mobilized contaminant cannot be controlled and may migrate down through the aquifer rather than being pumped out at the producing well. The effects of mobilization and solubilization on trapped residual organic phases need to be understood so that the more efficient process of mobilization can be used when safely possible.[6] The complex interactions that occur in the subsurface environment require a better understanding so that field applications can be designed for maximum efficiency.

## Numerical Modeling

There has been a great deal of work in modeling subsurface fluid flow reported in both the petroleum and groundwater literature. Efforts to model surfactant enhanced aquifer remediation intensified in the early 1990's. Most of the work reported so far has been limited in some aspect. Brown

and Pope (1994) report by far the most comprehensive modeling to date. They developed a general SEAR model that incorporates multiphase behavior and includes the effects of interfacial tension reduction and phase behavior. The model is three dimensional and is capable of including the heterogeneous distribution of aquifer properties.[11]

Prior to the work of Brown, Pope, *et al.*, (1994) and Delshad, *et al.*, (1994), the work reported was limited to single phase flow solubilization (omitting the effect of mobilization through reduced IFT).[11] Wilson (1989) and Wilson and Clark (1991) developed a 2-D areal single phase model.[11] In this model, they assumed local equilibrium of all the components and constant isotropic permeability. This model also limited the chemical reaction to absorption of surfactant and solubilization of the contaminant. Abriola, *et al.*, (1993)[11] developed a 1-D, single phase simulator that modeled the solubilization process emphasizing rate limited mass transfer.

Brown and Pope's work is based on a general, finite difference model, UTCHEM, originally developed to model surfactant enhanced oil recovery.[12] Modifications to this enhanced oil recovery model by Delshad, *et al.*, (1995)[13] allow it to be used to model surfactant enhanced aquifer remediation. The modifications include nonequilibrium mass transfer, NAPL solubility in water, constant potential surface boundary, primary drainage capillary pressure and relative permeability.[13] The model is a finite difference

reservoir simulator that solves discrete mass balance equations for each component in the system. The 1994 work by Brown and Pope studied a single heterogeneous aquifer and examined the sensitivities to contaminant concentration, pumping rate, and spatial discretation.

Although the results reported by Brown and Pope were very encouraging, they were unable to compare their results to actual field cases because there was little data at the time. Later work by Intera Corporation, applied the UTCHEM SEAR model to a field study. In this study, the field data agreed very well with that predicted by UTCHEM.[14]

The primary disadvantage of the work reported by Brown and Pope is the computer time required for a simulation. Three dimensional simulations required between 5 minutes and 3 hours of CPU time on a CRAY Y-MP, depending on the discretization and number of dimensions considered. The use of a PC (486SX) increased simulation times by an order of magnitude. Computation time will increase significantly for fine scale applications incorporating fine scale heterogeneity geostatistical descriptions. Due to the very long simulation times, numerical simulation may prove to be unfeasible to study alternative scenarios, for process optimization, and to quantify uncertainty.

Excellent reservoir simulation results are reported using a semi-analytical streamline model reservoir simulator.[15] The model that this

simulator is based on relies on the observation that in a velocity field derived by finite difference, streamlines are approximated by piecewise hyperbolic segments. This speeds up the solution time because the finite difference equation needs only to be solved once to define the velocity distribution. Once the velocity distribution is known, for example, the phase saturation distribution along streamlines may be calculated analytically using the well known Buckley-Leverett frontal advance equation.[15]

# CHAPTER III

## METHODS

### Overview

The procedure to formulate and validate the streamline based simulator for surfactant enhanced NAPL remediation is divided into three distinct steps.

1. Understand the current state of the art in SEAR simulation by studying the sensitivity of UTCHEM to changing aquifer properties. The results of the UTCHEM simulations will be used as a benchmark to judge the performance of the streamline model.

   - Select a geometry that is representative of a field case and use UTCHEM to simulate surfactant enhanced remediation.

   - Change aquifer properties systematically to study the sensitivity of the model to changes in longitudinal and transverse dispersivity, injected surfactant/polymer concentration and aquifer heterogeneity.

2. Apply fractional flow theory to simulate surfactant effects in a 3-D streamline based aquifer simulator.

- Modify the code of an existing two phase streamline aquifer simulator to incorporate surfactant effects. The two main effects modeled are mobilization and solubilization. The modifications will include the effect of surfactant on residual NAPL saturation, relative permeability curves and hence, the fractional flow curves.

- Mobilization by the reduction of interfacial tension between the phases is modeled through the resulting changes in the low tension fractional flow curves. Changes in relative permeability curves results in the formation of two shock fronts. The additional shock fronts are incorporated into the model to calculate the amount of NAPL produced.

- Fractional flow theory as applied to surfactant injection assumes there is no transfer of surfactant to the NAPL. Solubilization is modeled through partitioning coefficients that estimate the mass transfer between the phases. It also assumes that the concentrations are sufficiently low so that the volume fraction of the surfactant is negligible in the aqueous phase.[8,16]

3. The sensitivity studies made with UTCHEM are then repeated with the streamline model.

- Compare results to show that the effects of surfactant are captured adequately using the fractional flow approximation.

- Compile and run the streamline model on a SPARC Workstation, a desktop PC and a laptop PC. Compare run times to show that the streamline model can easily be used in the field to design applications.

### Benchmark

As mentioned above, UTCHEM was selected for use as a benchmark to judge the performance of the newly developed streamline model. UTCHEM (version 5.32M 1995) is comprehensive in its accounting for a wide variety of chemical effects as well as aquifer heterogeneities. In UTCHEM, the pressure is solved for implicitly and concentrations are solved for explicitly. Phase saturations and concentrations are then solved in a "flash" routine which incorporates thermodynamic phase equilibrium. This model has been tested in the field with good results.[14] The details of this simulator and tests are reported extensively in the literature.[11,13,14]

To begin the study, an aquifer geometry, average aquifer and average surfactant and polymer parameters were selected that are representative of other studies and field cases. The work of Intera Corporation[14] provided the geometry and average aquifer properties. A unit cross section 25 ft. long and 22 ft. deep was selected to model a suspected contamination at USAF Plant 4, Fort Worth, Texas. The work of Brown, *et al.* (1994)[11] provided relevant surfactant and polymer properties. **Table 1** summarizes the average aquifer

| TABLE 1 – AQUIFER AND CHEMICAL PARAMETERS USED IN SIMULATIONS | |
|---|---|
| Parameter | Value |
| Average permeability | 1.0 Darcy |
| Anisotropy ratio ($k_{zz}/k_{xx}$) | 0.1 |
| Average porosity | 0.35 |
| Longitudinal dispersivity | 1.0 ft |
| Transverse dispersivity | 0.1 ft |
| Residual Water saturation | 0.25 |
| Residual NAPL saturation | 0.20 |
| Interfacial tension | 45 dynes/cm |
| Water viscosity | 1 cp |
| NAPL viscosity | 0.9 cp |
| Relative permeability endpoints | 0.49 water<br>0.65 NAPL<br>0.49 surfactant |
| Corey Function exponents | 2.85 water<br>2.65 NAPL<br>2.85 surfactant |
| Surfactant | sodium diamyl/dioctyl sulfosuccinate |
| Surfactant sorption | $1.0045 \times 10^{-3}$ vol. Surf./pore vol. |

parameters and relevant chemical properties selected for use in this study.

The effect of changes to several aquifer parameters were examined in this study. The most important of these parameters is probably aquifer permeability.[6] Three random permeability fields were created using a sequential Gaussian simulator in *GSLIB: Geostatistical Software Library and User's Guide*.[17] The fields differed in the correlation length selected for generating the permeability fields. The three lengths used for this study were 1 ft., 5 ft., and 10 ft., which corresponds to 4%, 20%, and 40% of the principle flow direction. A base case of a homogeneous aquifer was selected with a permeability of 1000 md. Each of the random heterogeneous permeability fields were generated assuming an average permeability of 1000 md and a lognormal distribution with a variance of 1. Contour plots of the three fields are shown in **Fig. 1**. Note that the permeability field generated with a 1 ft. correlation length is almost completely random. As the correlation length increases, the connectivity, especially of the low permeability channels, increases. The effect of the channeling will be apparent in the production histories that follow. Most noticeable is a decrease in time to breakthrough in the production histories that is captured by both the streamline model and UTCHEM. This effect is more pronounced in the streamline model than in the UTCHEM model in the simulations of this study.

Fig. 1 – Random permeability fields created with sequential Gaussian algorithm in GSLIB.

In addition to the effect of permeability, other parameters selected for examination include changes in longitudinal and transverse dispersivities, and the effect of adding polymer to the injection fluid. For the initial sensitivity analysis with UTCHEM, dispersivities are varied by two orders of magnitude. The base case dispersivity for all of the simulations was taken as 1 ft. for the longitudinal dispersivity and .1 ft. for the transverse dispersivity. Injected polymer varies from 0% to .5%. Most of the simulations were run at a base case of 0% injected polymer. Results of these studies and comparisons to the history output from the modified streamline model follow.

## Fractional Flow Theory

Fractional flow theory applied to surfactant enhanced remediation begins with the Buckley-Leverett frontal advance theory for waterflooding. The details of the theory are discussed thoroughly in the literature and only an outline of its application to SEAR is provided below. For a thorough discussion, see references (8) and (16). The following assumptions are implicit in the application of the frontal advance theory to this problem.[16] Several of the assumptions are relaxed to apply fractional flow theory to more general cases.

- One dimensional flow in a homogeneous, isotropic, isothermal aquifer

- At most two phases are flowing

- At most three components are flowing

- Local equilibrium exists

- The fluids are incompressible

- The adsorption isotherm depends only on one component and has negative curvature

- Dispersion and capillarity are negligible

- No viscous fingering occurs

- Darcy's law applies

- The initial distribution of fluids is uniform

The case of a three component, two-phase flood can be applied to a surfactant flood. In this case, the differential material balance equation for any component, i, in two phase flow is[16]

$$\frac{\partial}{\partial t}(C_{i1}S_1 + C_{i2}S_2 + \hat{C}_i) + \frac{q_t}{A\phi}\frac{\partial}{\partial X}(C_{i1}f_1 + C_{i2}f_2) = 0 \dots\dots\dots\dots (1)$$

Note that $C_{ij}$ represents the concentration of component i in phase j and $\hat{C}$ represents the adsorption of each component on aquifer rock. For this study, component i = 1,2,3 (water, NAPL, and surfactant) and phase j = 1,2 (water

rich and NAPL rich). Polymer, when present, is assumed to travel with the aqueous phase and alter its viscosity. Thus polymer transport is not explicitly modeled. The solution of this equation indicates the formation of a "shock front" wherever the saturation velocities upstream are greater than downstream. This is true for most water-NAPL fractional flow curves. An overall material balance gives the velocities of the shock fronts (the saturation discontinuities).

**Fig. 2** is a schematic of NAPL saturation profiles at a given time. Note in the following discussions that $S_{wb} = S_1' = (1 - S_{ob})$, $S_1'' = (1 - S_{obt})$ and $S_{orw} = (1 - S_{wi})$. Assuming that the shock fronts are self-sharpening, there
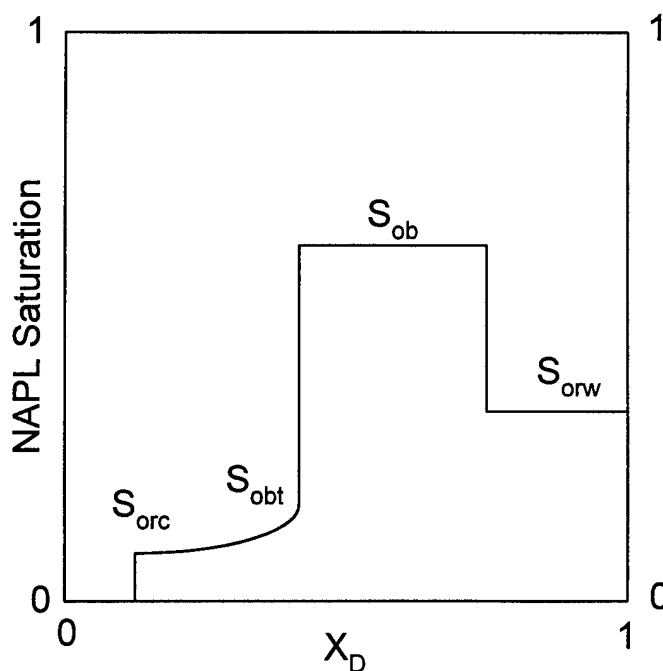


Fig. 2 – NAPL saturation profile, miscible displacement.

are three distinct regions of different phase compositions.[18] Downstream, there is only NAPL and water, upstream there is the injected composition. In between there is a surfactant shock. At the front of the NAPL bank, a shock front is formed between the water and the NAPL. At this point, the water saturation changes abruptly from the initial saturation to the NAPL bank saturation ($S_{wi}$ to $S_{wb}$). The velocity of this front is given by

$$v_{\Delta C_1} = \frac{q}{A\phi} \frac{f_{wi} - f_{wb}}{S_{wi} - S_{wb}} \quad\text{...................................................................} (2)$$

From Eq. 1, the velocity of any saturation in a two-phase flow region of constant concentration is

$$v_{S1} = \frac{q}{A\phi} \frac{df_1}{dS_1} \quad\text{.......................................................................} (3)$$

By making a material balance across the surfactant shock front, Pope (1980)[16] finds this surfactant front velocity to be

$$v_{\Delta C_i} = \frac{q}{A\phi} \frac{(C''_{i1}f''_1 - C'_{i1}f'_1) - (C''_{i2}f''_1 - C'_{i2}f'_1) + C''_{i2} - C'_{i2}}{(C''_{i1}S''_1 - C'_{i1}S'_1) - (C''_{i2}S''_1 - C'_{i2}S'_1) + C''_{i2} - C'_{i1} + \hat{C}''_i - \hat{C}'_i} \quad\text{......................} (4)$$

where the double prime indicates upstream values and the single prime indicates downstream values. Eq. 4 is then solved for velocity downstream where the concentration of the surfactant (component 3) is 0. The solution is

$$v_{\Delta C_3} = \frac{q}{A\phi} \frac{f''_1 + b}{S''_1 + a} \quad\text{...............................................................} (5)$$

where

$$b = \frac{C_{32}''}{C_{31}'' - C_{32}''} \quad \dots\dots\dots\dots\dots\dots\dots\dots\dots\dots\dots\dots\dots\dots\dots\dots\dots\dots\dots\dots\dots\dots\dots\dots \quad (6)$$

and

$$a = \frac{C_{32}'' - \hat{C}_3''}{C_{31}'' - C_{32}''} \quad \dots\dots\dots\dots\dots\dots\dots\dots\dots\dots\dots\dots\dots\dots\dots\dots\dots\dots\dots\dots\dots\dots\dots \quad (7)$$

As in Eq. 3, the velocity of any saturation in a two phase flow region in an area of constant concentration is

$$v_{S_1} = \frac{q}{A\phi} \frac{df_1}{dS_1} \quad \dots\dots\dots\dots\dots\dots\dots\dots\dots\dots\dots\dots\dots\dots\dots\dots\dots\dots\dots\dots\dots\dots\dots\dots \quad (8)$$

At a saturation $S_1''$, $v_{\Delta C_3}$, and $v_{S_1}$ are equal, so equating Eqs. 5 and 8,

$$\frac{f_1'' + b}{S_1'' + a} = \left. \frac{df_1}{dS_1} \right|_{S_1 = S_1''} \quad \dots\dots\dots\dots\dots\dots\dots\dots\dots\dots\dots\dots\dots\dots\dots\dots\dots\dots\dots\dots \quad (9)$$

This equation is solved graphically by drawing a line from (–a,–b) tangent to the low tension fractional flow curve. The tangent point gives the values for $\left(S_1'', f_1''\right)$.

The saturation in the NAPL bank is found by applying Eq. 4 to a second component and then eliminating $f_1''$ and $S_1''$. This result is

$$v_{\Delta C_2} = \frac{f_1' + d}{S_1' + c} \dots\dots\dots\dots\dots\dots\dots\dots\dots\dots\dots\dots\dots\dots\dots\dots\dots\dots\dots (10)$$

where

$$d = C_{22}'' - 1 - b(C_{21}'' - C_{22}'') \dots\dots\dots\dots\dots\dots\dots\dots\dots\dots\dots\dots\dots (11)$$

and

$$c = C_{22}'' - 1 - a(C_{21}'' - C_{22}'') \dots\dots\dots\dots\dots\dots\dots\dots\dots\dots\dots\dots\dots (12)$$

As in above, at the shock front, at a saturation $S_1'$, $v_{\Delta C_2}$, and $v_{S_1}$ are equal, so



Fig. 3 – Graphical solution to Eq. 9 and Eq. 13.

$$\frac{f_1' + d}{S_1' + c} = \frac{df_1}{dS_1}\bigg|_{S_1 = S_1'} \quad\text{.............................................................................................(13)}$$

This equation is solved graphically as before by drawing a line parallel to the above tangent and passing through the point $(-c, -d)$. The intersection of the straight line with the high tension fractional flow curve gives the value of $(S_1', f_1')$, the NAPL bank saturations and fractional flow. **Fig. 3** illustrates the graphical solution of Eq. 9 and Eq. 13. Note that for certain injected compositions is a second surfactant shock is formed where the NAPL saturation will go to zero.[16] This is not modeled in this simulator.

The composition varies from an initial constant saturation of $S_{or}$ to a constant NAPL bank saturation $S_{ob} = (1 - S_1')$. After the end of the NAPL bank, a continuous decrease in NAPL saturation occurs at fixed phase concentration until the residual NAPL saturation with surfactant is reached $(S_{orc})$. After breakthrough of the surfactant, the rate of recovery is given by the typical Welge integration, including the effect of the partitioning between the NAPL between the aqueous phase and the microemulsion phase (see also **Fig. 2**).

The time required to reach each of the stages is given by the inverse of the derivatives of the fractional flow with respect to saturation,

$$t_D = \left(\frac{df_1}{dS_1}\right)^{-1} \dots\dots\dots\dots\dots\dots (14)$$

For the time to arrival of the NAPL bank, the time is given by

$$t_{D1} = \frac{S_1' - S_{wi}}{f_1' - f_{wi}} \dots\dots\dots\dots\dots\dots (15)$$

For tertiary recovery, $S_{wi} = 1 - S_{or}$, and $f_{wi} = 1$.

The time to arrival of the end of the NAPL bank comes from Eq. 7,

$$t_{D2} = \frac{S_1'' + a}{f_1'' + b} \dots\dots\dots\dots\dots\dots (16)$$

For tertiary recovery, the amount of organic phase recovered before arrival of the NAPL bank ($t_D < t_{D1}$) is

$$N_p = 0 \dots\dots\dots\dots\dots\dots (17)$$

During the NAPL bank, ($t_{D1} \leq t_D \leq t_{D2}$), the recovery is at a constant saturation given by

$$N_p = (1 - f_1')t_D \dots\dots\dots\dots\dots\dots (18)$$

After breakthrough of the surfactant, the production continuously decreases until $S_{orc}$ is reached. The production is calculated by

$$N_p = \left[C_{22}''(1 - f_1') + C_{21}'' f_1'\right]t_D \dots\dots\dots\dots\dots\dots (19)$$

This equation accounts for the NAPL in the oleic phase ($C_{22}''$) and the NAPL in the aqueous phase ($C_{21}''$).

## Partitioning Coefficients

It is often convenient to express the above relationships in terms of partitioning coefficients. We will make several definitions following the convention of Larson (1978)[18] to describe the mass transfer in the system. Assumptions implicit in this model in addition to those assumed for fractional flow theory include:

- Each of the three components behave as if each are pure

- Mass transfer of surfactant, water and NAPL between the mobile phases is allowed as well as the transfer of the surfactant to the aquifer rock

- There are no chemical reactions

- Each component occupies the same volume as it would have in its pure state (no excess volume of mixing)

- Endpoint relative permeabilities, residual saturations and exponents are functions of composition only

- Fluid properties, especially viscosity, depend only on composition

- The injected fluid is a single aqueous phase of constant composition

- Porosity is not affected by absorption of surfactant or fluid flow rate

We assume that the mass transfer is described adequately by four parameters, $D_s$, $k_c$, $k_{oo}$, and $k_o$. $D_s$ is the frontal lag resulting from the adsorption of surfactant on the rock. The units are (pore volumes of lag) / (pore volumes of fluid injected). $D_s$ is calculated by equating the total volume of surfactant injected to the total absorbed.[10]

$$D_s = \left(\frac{1-\phi}{\phi}\right)\left(\frac{\rho_r a_s}{\rho_s C_s}\right)\frac{1}{1000} \quad \dots\dots (20)$$

Where $a_s$ is the surfactant retention in (mg surfactant)/(g rock), and $C_s$ is the concentration of the injected surfactant. Expressed in terms of Eq. 4,

$$D_s = \frac{\hat{C}_3}{C_{31}} \quad \dots\dots (21)$$

The partition coefficient, $k_c$, is the ratio of the concentration of chemical in the oleic phase that would be in equilibrium with the aqueous phase to the concentration of chemical in the aqueous phase.

$$k_c = \frac{C_{32}}{C_{31}} \quad \dots\dots (22)$$

$k_{oo}$ is the concentration of the NAPL in the equilibrium oleic phase. Then $1 - k_{oo}$ is a measure of the swelling of the oleic phase with the chemical and water.

$$k_{oo} = C_{22} \quad \text{.................................................................................................(23)}$$

$k_o$ is the ratio of the concentration of NAPL in the injected aqueous phase to the concentration of NAPL in the equilibrium oleic phase. Of the partition coefficients defined, this is least likely to remain constant. The swelling coefficient, a measure of solubilization, is actually a function of surfactant concentration. This concentration will change during the history of a flood. The assumption that it remains constant simplifies the coding and provides reasonably accurate results in the simulations that follow. Finally, define

$$k_o = \frac{C_{21}}{C_{22}} \quad \text{..............................................................................................(24)}$$

Substituting these definitions into Eqs. 6, 7, 11, and 12 gives

$$a = \frac{k_c + D_s}{1 - k_c} \quad \text{.........................................................................................(25)}$$

$$b = \frac{k_c}{1 - k_c} \quad \text{.............................................................................................(26)}$$

$$c = k_{oo} - 1 - \left( \frac{k_c + D_s}{1 - k_c} \right) k_{oo} (k_o - 1) \quad \text{....................................................(27)}$$

$$d = k_{oo} - 1 - \left(\frac{k_c}{1 - k_c}\right) k_{oo} (k_o - 1) \dots\dots\dots\dots\dots\dots\dots\dots\dots\dots\dots\dots\dots\dots\dots\dots\dots\dots\dots\dots\dots (28)$$

## Phase Behavior

As mentioned previously, the formation of micelles is a strong function of salinity. In surfactant flooding, with low brine salinity, a typical surfactant is easily solubilized by the aqueous phase and poorly absorbed in the oleic phase. So at low salinity, a surfactant flood will have two phases at the surfactant front, a oleic phase that is almost pure NAPL and a microemulsion phase that is composed of brine, surfactant and a small amount of solubilized NAPL. This type of phase behavior is commonly referred to as type II(–) system or Winsor type I system.[8]

For a system of high salinity, the system again splits into two phases. This time, the phases consist of an aqueous phase of almost pure brine and a microemulsion phase of most of the surfactant and NAPL and some solubilized brine. This type of phase behavior is typically referred to as a type II(+) system or Winsor type II system.[8]

At intermediate salinities, a continuous change between the type II(–) and the type II(+) systems observed. At some salinity, there are three phases observed, an aqueous phase of almost pure brine, an oleic phase of almost pure NAPL and a microemulsion phase. This type of phase behavior

is know as a type III system or Winsor type IV system.[8] This system has almost unlimited solubility of NAPL and is perhaps the most efficient region for SEAR. Behavior of surfactants and NAPLs are not well understood in this region, however. The phase behavior becomes very complex.

The simulations of this study were constrained to lie within the type II(–) region. This is a justified because of the low salinity environment typically encountered in subsurface aquifer remediation. A type II(–) phase behavior ensures miscible displacement with the chase fluid and thus minimizes phase trapping.

## Streamline Modeling

A streamline numerical reservoir model was selected because of its computational efficiency without any significant loss in accuracy.[15] The reservoir model is semianalytic in that the velocity field is derived only once by a conventional finite difference fluid flow simulator. Once the velocity field is known, the streamlines are approximated by piecewise hyperbolic intervals. Along each of these intervals, the transport equation can be solved exactly. In particular, for multiphase and multicomponant flow, the semianalytic method first computes tracer transit times along streamlines and then solves the transport equations analytically in travel time coordinates. This approach captures the effects of heterogeneity with a great

deal of accuracy and is much faster than conventional methods. Following is an outline of the mathematical formulation used by the streamline model. For additional detail, readers are referred to Datta-Gupta and King (1995).[15]

In a nondeformable permeable media, the velocity field will be divergence free. Thus

$$\vec{\nabla} \cdot \vec{v} = 0 \quad \dotfill \quad (29)$$

and

$$\vec{v} = -\lambda \nabla p \quad \dotfill \quad (30)$$

as given by Darcy's law. The mobility $(\lambda = k / \mu)$ may be a function of position and $\vec{v}$ is the Darcy velocity. The velocity field is obtained first through a finite difference solution of Eq. 29. The trajectory of a particle injected into this velocity field is obtained by integrating

$$dT = \frac{dt}{\phi} = \frac{dx}{v_x} = \frac{dy}{v_y} = \frac{dz}{v_z} \quad \dotfill \quad (31)$$

In a finite element representation of a standard lowest order finite difference solution, the velocity varies linearly through each grid block and each velocity depends only on its own coordinates. Thus the velocity in Eq. 31 will be given by

$$v_i = b_i + c_i x_i \qquad i = 1,2,3 \quad .................................................................. \quad (32)$$

where the subscript i refers to the coordinate direction. Eq. 31 may be integrated exactly. The constants of motion, $b_i$ and $c_i$, are determined from Eq. 32 and the velocity field given by the finite difference solution.

In three dimensions, particle trajectories can be related to the bi-stream functions by[19]

$$\frac{\vec{v}}{\phi} = \nabla \psi \times \nabla \chi \quad .................................................................. \quad (33)$$

For example, in two dimensional flow in x and y, Eq. 33 becomes

$$\frac{\vec{v}}{\phi} = \nabla \psi \times \hat{z} \quad .................................................................. \quad (34)$$

where $\hat{z}$ is the unit vector in the z direction. A bilinear form of the stream function given by

$$\psi = \psi_0 + ax + by + cxy \quad .................................................................. \quad (35)$$

is consistent with linear velocities

$$v_x = (b + cx); \quad v_y = -(a + cx) \quad .................................................................. \quad (36)$$

In three dimensions, the solution of Eq. 31 takes the form of two independent relationships that represents two families of surfaces whose

intersections are the streamlines. Mathematically, these surfaces are described by

$$\omega = \omega(x,y,z) = \text{const.}; \quad \chi = \chi(x,y,z) = \text{const.} \quad \dots\dots\dots (37)$$

The functions $\omega$ and $\chi$ are called the stream functions of three dimensional flow. Along each streamline, the stream functions are constant. The streamline is thus a characteristic curve of Eq. 31. The solution to Eq. 31 then becomes[19]

$$v_x = \left( \frac{\partial \omega}{\partial y}\frac{\partial \chi}{\partial z} - \frac{\partial \omega}{\partial z}\frac{\partial \chi}{\partial y} \right); \quad v_y = \left( \frac{\partial \omega}{\partial z}\frac{\partial \chi}{\partial x} - \frac{\partial \omega}{\partial x}\frac{\partial \chi}{\partial z} \right); \quad v_z = \left( \frac{\partial \omega}{\partial x}\frac{\partial \chi}{\partial y} - \frac{\partial \omega}{\partial y}\frac{\partial \chi}{\partial x} \right) \quad \dots (38)$$

Note that for flow in the x-y plane, the planes $z = \text{const.}$ are the stream surfaces and with $\omega = z$ and $\chi \equiv \Psi$, Eq. 38 reduces to Eq. 32.

A particle initially at a point $(x_0, y_0)$ will move according to Eq. 32. The trajectory is calculated by direct integration of Eq. 31. In the x direction, this becomes

$$\int \frac{dx}{b + cx} = \int \frac{dt}{\phi} = \int dT \quad \dots\dots\dots\dots (39)$$

which results in

$$v_x = v_x(x_0)\exp(cT) \quad \dots\dots\dots\dots (40)$$

$$x = x_0 + v_x(x_0)(\exp(cT) - 1)/c \quad \dots\dots\dots\dots (41)$$

in the x direction. In the y direction, the solution is

$$v_y = v_y(y_0)\exp(-cT) \hspace{4cm} (42)$$

$$y = y_0 + v_y(y_0)(1 - \exp(-cT))/c \hspace{3cm} (43)$$

Similar equations apply in the z direction for three dimensional flow.

Transit time information is used to calculate transport phenomenon through the porous media. The travel time across a grid block is obtained from the integration of Eqs. 38 and 39.[20] For example, in the x direction, the time required to move from $x_0$ to any location x is

$$-\int_{x_0}^{x} \frac{dx}{b+cx} = \Delta t_s \hspace{4cm} (44)$$

$$\ln\left[\frac{(b+cx)}{(b+cx_0)}\right] = -c\Delta t_x \hspace{3cm} (45)$$

The actual travel time across a gridblock will be the minimum positive across all allowable faces.[15] The time of flight to any location ($x_0,y_0$) is obtained by following the streamline backwards in time to the injector through successive grid blocks in the finite difference model and summing the times through each grid block. The streamline model uses a standard finite difference techniques to solve for velocities in each grid block. This solution provides values of normal velocity on each grid block face and fixes

the values of the constants a, b, and c in the previous equations. Because the streamlines must enter and exit through grid block faces, the actual transit time across a grid block is given by the minimum over the allowed edges.[20] This calculation is repeated through each grid block until the injector is reached. The sum of the transit times across grid blocks define the function $\tau(x,y)$ where (x,y) is the point the calculation begins. If the trajectory begins at the producer, the transit time can be labeled as a function of streamline, $\tau(\psi)$. This function is used to calculate the recovery histories at the producing wells. Note that this analysis applies equally in three dimensions even though the above discussion is in two dimensions.

The above described semianalytic method can be applied to the calculation of saturation distributions assuming that the appropriate one-dimensional solutions exist along a streamline. The method of applying the previously discussed transit time calculation is illustrated for a two-phase immiscible displacement. The method is easily extended to more complicated flow situations with little modification.

The equation describing the flow of two immiscible, incompressible phases is the general material balance equation[8]

$$\phi\frac{\partial S_w}{\partial t} + \vec{v}\cdot\nabla F(S_w) = 0 \quad\text{.................................................................}(46)$$

with the initial and boundary conditions defined by

$$S_w(x,0) = S_{wi} \quad\text{..........................................................................................} (47)$$

$$F(S_w(0,t)) = F_{w,inlet} \quad\text{..................................................................} (48)$$

where

$$F(S_w) = f_w = \frac{\lambda_w}{\lambda_w + \lambda_n} \quad\text{...............................................................} (49)$$

is the fractional flow of the aqueous phase. The $\lambda_w$ and $\lambda_n$ are the aqueous phase and NAPL phase mobilities respectively. The phase mobility is defined as

$$\lambda_j = kk_{rj}(S_w)/\mu_j \quad\text{...............................................................} (50)$$

where the subscript j indicates the phase. Note that the fractional flow is independent of the absolute permeability but is a strong function of the relative permeabilities. For constant phase viscosities, $\mu_w$ and $\mu_n$, the fractional flow of water is a function of water saturation, $S_w$, only. For the purposes of these simulations, it is assumed that the relative permeability has the following form

$$k_{rj} = k_r^0 S_{nj}^n \quad\text{...............................................................} (51)$$

where $S_{nj}^n$ is the normalized phase saturation. For example, the water phase

saturation is $S_{nw} = \dfrac{S_w - S_{wc}}{1 - S_{wc} - S_{or}}$. Eq. 46 can be rewritten in terms of $(\tau, \psi)$ as

the independent spatial variables. This results in

$$\frac{\partial S_w}{\partial t} + \frac{\partial F(S_w)}{\partial \tau} = 0 \quad\text{................................................................(52)}$$

The solution of Eq. 52 is given by

$$\frac{\tau(x,y)}{t} = \frac{dF(S_w)}{dS_w} \quad\text{....................................................................(53)}$$

The value of $f_w$ is a single valued function of $S_w$ only. Consequently, the

solution to the two-phase problem at any time is reduced to a trivial

calculation once the transit time to that location is known.

Using the transit time approach, the tracking and flow solutions can be

mapped along streamlines in three dimensions. Thus, the streamline transit

time approach provides a general framework for extending the fractional

flow solution to multidimensional situations. Since the velocity field is

derived numerically, the approach presented here can handle porosity and

permeability heterogeneity and arbitrary well configurations.

## Solution Outline

The following steps are used in the streamline based simulation.

- The velocity field is defined for the aquifer grid based on a standard finite difference solution of Eq. 29.

- Streamline trajectories are determined from the producer back to the injector by solution of Eq. 31. The number of streamlines is input by the user. From this, transit times along a streamline are determined to each grid block ($\tau(x,y)$).

- Digitized fractional flow curves and their derivatives are created for both low tension and high tension cases based on user input. Breakthrough of surfactant is determined by the graphical solution of Eqs. 9 and 13 (see also **Fig. 3**).

- At fixed time steps at each grid block, the production stage is determined from solution of Eqs. 14, 15, and 16 using the streamline transit time, $\tau(x,y)$ at this producer, and Eq. 53. Eq. 53 is used to compute the arrival times at the producer for saturation fronts from the relationship $t = \tau / dF(S_w) / dS_w$. If the time step, t, is less than $t_{D1}$, NAPL production is given by Eq. 17. If the time is within the NAPL bank ($t_{D1} \leq t_D \leq t_{D2}$), production is given by Eq. 18. If the time is after breakthrough of the surfactant, NAPL production is given by Eq. 19. The total production from each grid block is summed and averaged for the total production during each time step.

- The saturation profile is generated grid block by grid block in a process similar to the production algorithm. At a user defined time, for each grid block, the saturation stage is determined from solution of Eqs. 14, 15, and 16 using the streamline transit time, $\tau(x,y)$, and Eq. 53 as in the previous step.

- If the time is before the arrival of the NAPL bank, the saturation of that block is assumed to be $S_{wi}$. If the time is during the NAPL bank, the saturation is assumed to be $S_{ob}$. If the time is after surfactant breakthrough, the saturation is assumed to be in the "tail" of the low tension fractional flow curve and the program interpolates a saturation value based on the low tension fractional flow curve and the transit time to that grid block.

# CHAPTER IV

# RESULTS AND DISCUSSION

## Calibration

The emphasis of this study is to develop new computer code that predicts the performance of surfactant enhanced aquifer remediation. Since the amount of field data is extremely limited, the new code will be validated in terms of its ability to reproduce the results of a high resolution finite difference simulator. As mentioned previously, the finite difference simulator selected is UTCHEM v5.32. This simulator has been adapted to surfactant remediation by others and its ability to predict behavior of SEAR projects in the field has been reported in the literature.[11,14]

Multiphase flow in general and fractional flow theory in particular is extremely sensitive to relative permeability curves. Consequently, for accurate comparison of the two models, both simulators must use the same model for the relative permeability, Eq. 51. The streamline model was designed so that both simulators use the same relative permeability endpoint, residual saturation and exponents in the model equations in the high tension case. **Fig. 4** is a graph of the output from both simulators
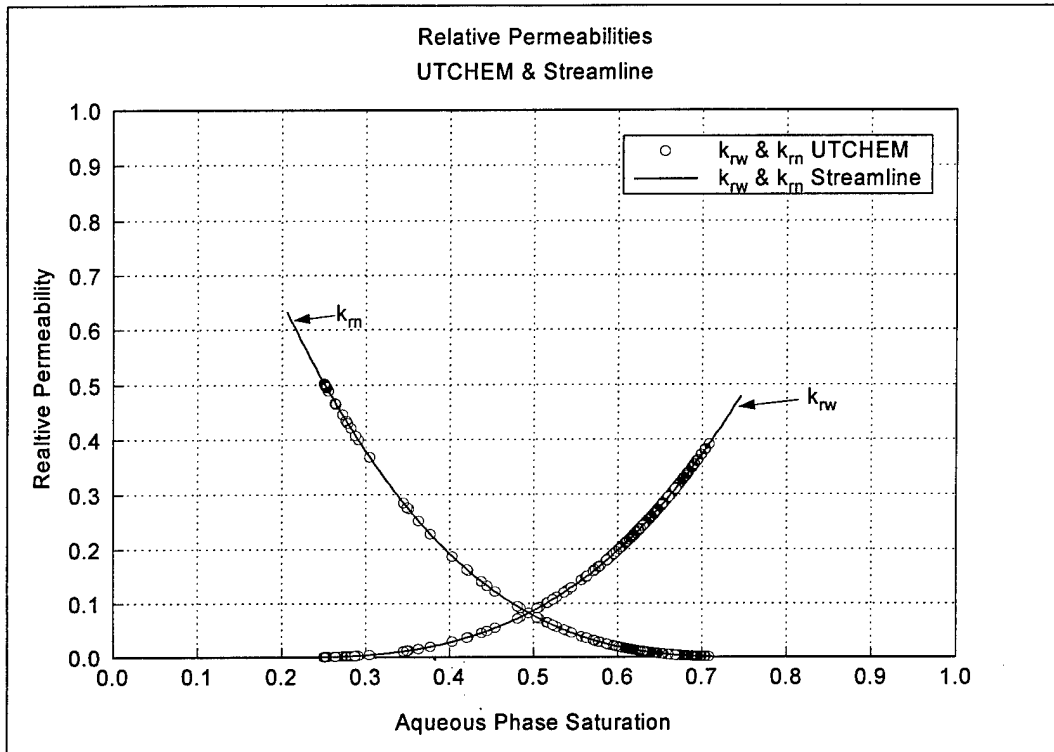
Fig. 4 – Relative permeability curves from UTCHEM and streamline models used for simulations.

illustrating that the relative permeability curves generated by each are identical.

After ensuring that the relative permeability curves in both simulators are the same, a simple water flood simulation was run to see if the production history curves for the simulators were similar. For this simulation, both a homogeneous aquifer and a heterogeneous aquifer with a long correlation length were used. **Fig. 5** presents production histories for UTCHEM and the streamline model. Note that the divergence in the histories increases with increasing heterogeneity.
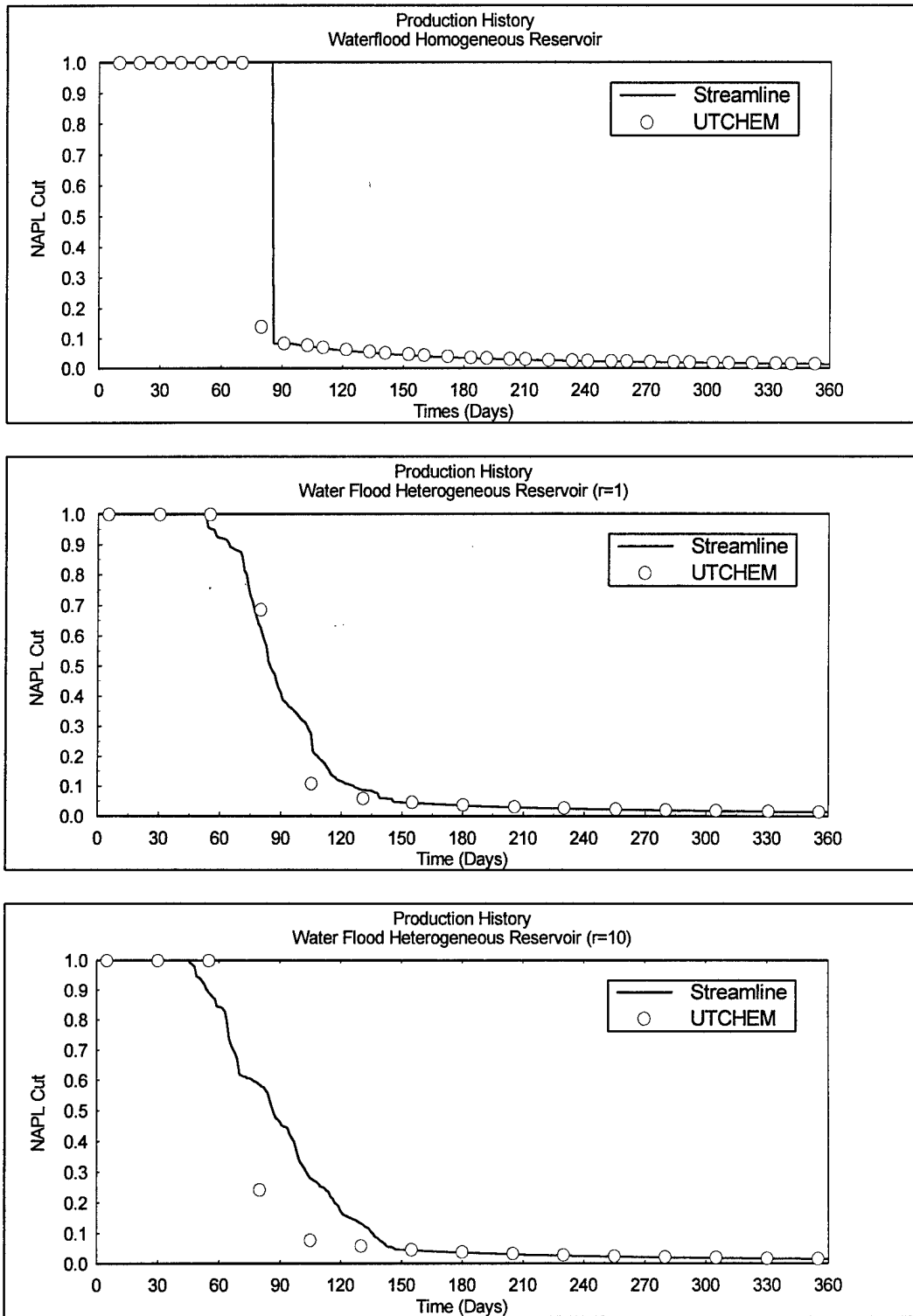
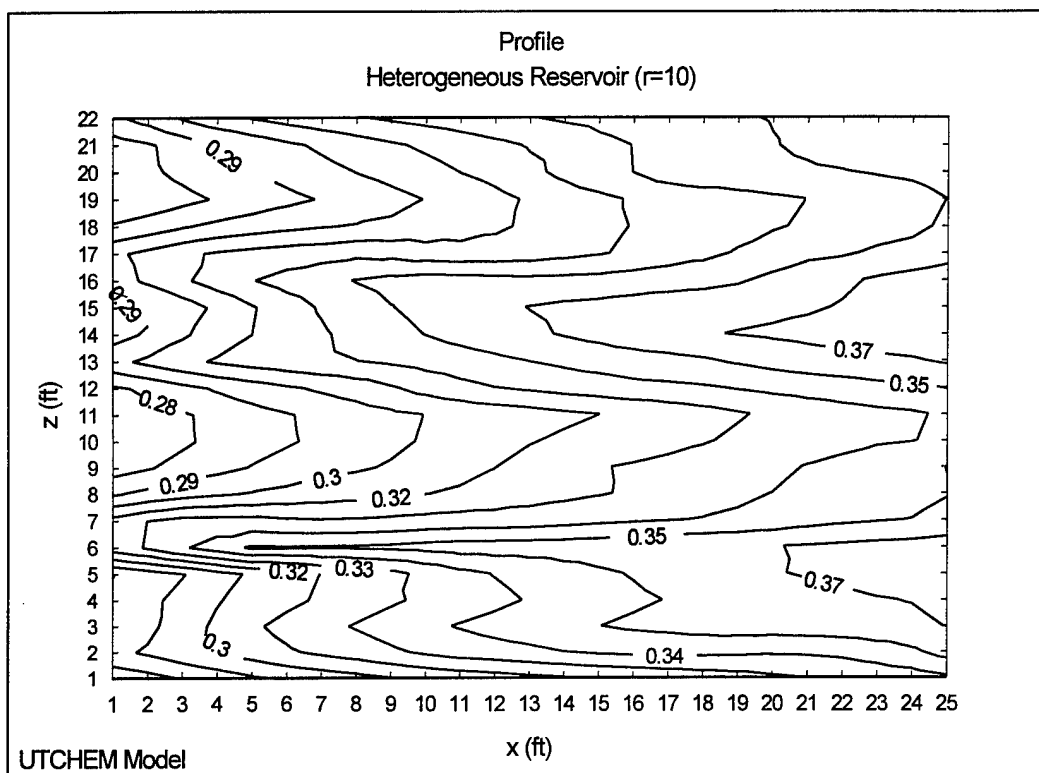Fig. 5 – Production history curves for water flood calibration tests.
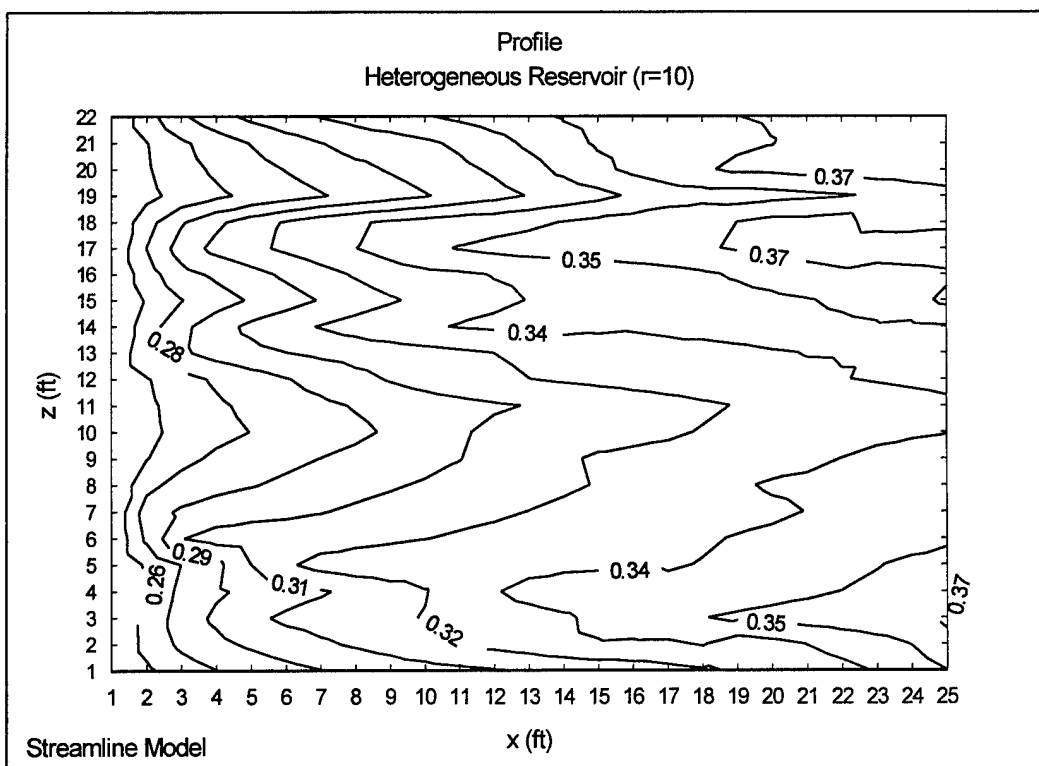
Fig. 6 – Aquifer profiles from waterflood calibration simulations.

This divergence of the simulators with increasing is also seen by examining the aquifer profiles presented in **Fig. 6**. This figure is a contour plot of the residual NAPL distribution after 365 days of water flood in an $r = 10$ aquifer. The profile of the $r = 1$ aquifer is similar, except that its residual saturation is slightly lower. Although the general shape and residual NAPL saturation produced from either simulator is similar, the match is not perfect. The effect becomes even more pronounced when surfactant is added as will be shown in the discussions that follow. This may be caused because the streamline model is not as capable of capturing the effects of the interaction of the flooding process with that of the heterogeneity.[20] Another possible cause of the difference is that the streamline model assumes that the velocity field remains constant. This is not strictly true. It is most likely that the streamline model better predicts the effects of channeling. Note that in **Fig. 5** the sharp channeling present in the streamline profile. The UTCHEM produced profile shows diffused channeling that increases from injector to producer.

## Polymer Effect

The addition of polymer to the injected fluid has long been recognized as an effective method of increasing the efficiency of water flooding and chemical flooding in enhanced oil recovery.[8] The benefits should equally apply to aquifer remediation.[11] Obviously, the choice of a polymer is much

more critical in aquifer remediation in terms of its toxicity and biodegradability. The polymer properties selected for the simulations are those of xanthan gum. Since xanthan gum is an FDA approved food additive, the concerns over contaminating the aquifer are reduced.

Polymer is effective in increasing the areal and sweep efficiency as well as the displacement efficiency. Fractional flow theory accounts for the increase in displacement efficiency.[16] The streamline model accounts for the areal sweep efficiency. One effect of injected polymer is the changing of the effective viscosity of the injected stream. This increased viscosity reduces the amount of NAPL that is bypassed by the injected fluid. Very little polymer is required to provide adequate mobility control. SEAR applications require an increase in injected fluid viscosity to about 5 cp for adequate mobility control. This corresponds to about a .05% polymer concentration.[6]

The use of injected polymer for mobility control is implemented in the streamline model by the effect of polymer on the viscosity on the injected fluid. However, polymer also has some effect on the phase behavior, adsorption and other properties of the surfactant/polymer mixture.[6] While these more detailed effects are not modeled in the streamline code, the simplified approach appears to be adequate in capturing most of the effects of polymer injection. The effect on phase behavior can be important if the polymer or water rich phase separates into one phase containing most of the
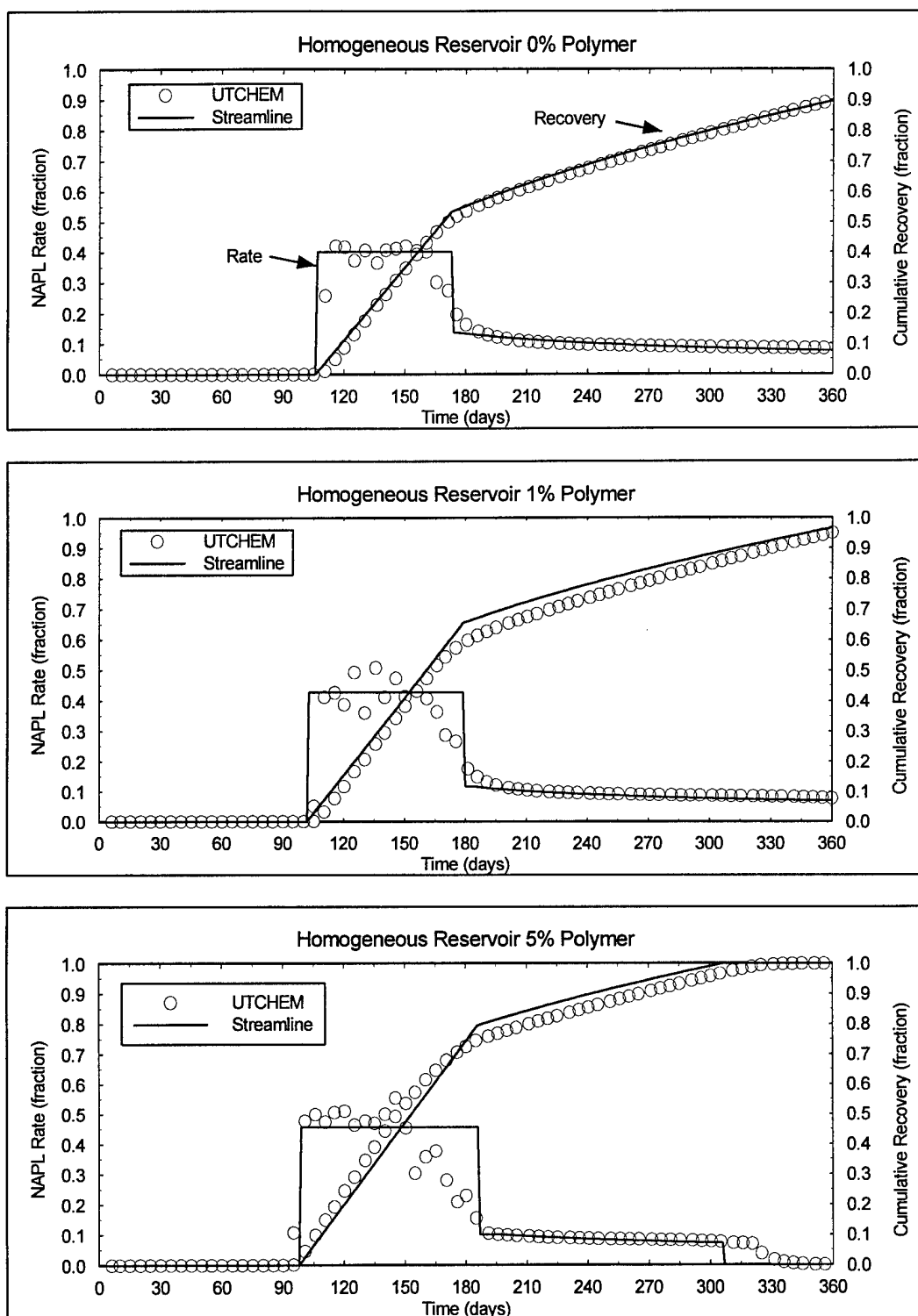
Fig. 7 – Production histories showing effect of increasing polymer concentration, UTCHEM and streamline models.

polymer and one phase containing most of the surfactant, which sometimes occurs.[6] There are other complexities involved with the addition of polymers that are not modeled in the streamline code. For example, this polymer has a non-Newtonian rheology where the apparent viscosity in the permeable medium is less than that measured in a bulk sample. Other examples of complexities include polymer adsorption, inaccessible pore volume, shear degradation, thermal stability, biodegradability, and electrolyte compatibilities.[6]

Because of the complexities that occur, especially with the phase behavior, that are not modeled in this version of the streamline code, most of the streamline simulations do not include a polymer. **Fig. 7** shows a sequence of production histories for both UTCHEM and streamline models in a homogeneous aquifer with no injected surfactant. There are two important items to note from these simulations. Most important is the very close agreement between the models. The streamline code matches very closely that of the high resolution finite difference code of UTCHEM and it does so in a fraction of the simulation time. A more detailed discussion of simulation time follows. In fact the streamline code arguably reproduces the theoretical production histories of a homogeneous reservoir better than UTCHEM. An examination of **Fig. 7** shows the numerical errors introduced by the finite difference methods of UTCHEM. A homogeneous aquifer

should produce a nearly perfect square wave, but the output of UTCHEM has rounded "shoulders". Additionally, there is some instability noticeable in the output from UTCHEM manifested in the "sawtooth" characteristics of the NAPL bank that probably could be reduced by decreasing the time step size.

Secondly, it is important to note that the addition of polymer, even very small concentrations, made significant improvements in the efficiency of the SEAR process. Although this is a widely recognized fact in enhanced oil recovery, the importance is less recognized by those involved in aquifer remediation technology.

### Heterogeneity

The effects of heterogeneity on the remediation process is the most difficult to model accurately. There are interactions between the heterogeneity and the flooding process that are not captured by the streamline method. Nevertheless, the effects of heterogeneity are captured with excellent accuracy. The ability of a SEAR simulator to accurately model heterogeneous aquifers quickly is also one feature that is often not included in other SEAR simulators. The streamline code is three dimensional, and is capable of modeling the anisotropic features of an aquifer. Although capable of modeling the anisotropic nature of

permeability, the simulations of this study were anisotropic only in the x-z direction.

In the simulations presented below, the aquifer is assumed to be isotropic in the x and y dimensions and have a constant z direction permeability equal to 10% of the average x-y dimension permeability. The simulations also do not include polymer, because the complex phase behavior that occurs with injected polymer masks the effects of the heterogeneity. From previous discussion, it is most likely that actual recovery will be much higher than that predicted by these simulations if polymer is included in the injected stream. Datta-Gupta, et al.[20], have shown the ability of the streamline code to accurately reproduce the effects of heterogeneity compared to field data. **Fig. 8** shows the ability of the streamline code to reproduce the effects of aquifer heterogeneity on production rate and cumulative production histories that are similar to the UTCHEM predictions.

The three permeability fields, as discussed earlier, are a sequence of randomly generated Gaussian permeability fields whose mean is constant but whose correlation length increases. The longer correlation lengths ( r = 5 ft. and r = 10 ft.) are not as well duplicated by the streamline model. These correlation lengths correspond to 4%, 20% and 40% respectively of the aquifer length. The longer correlation lengths show the effects of channeling
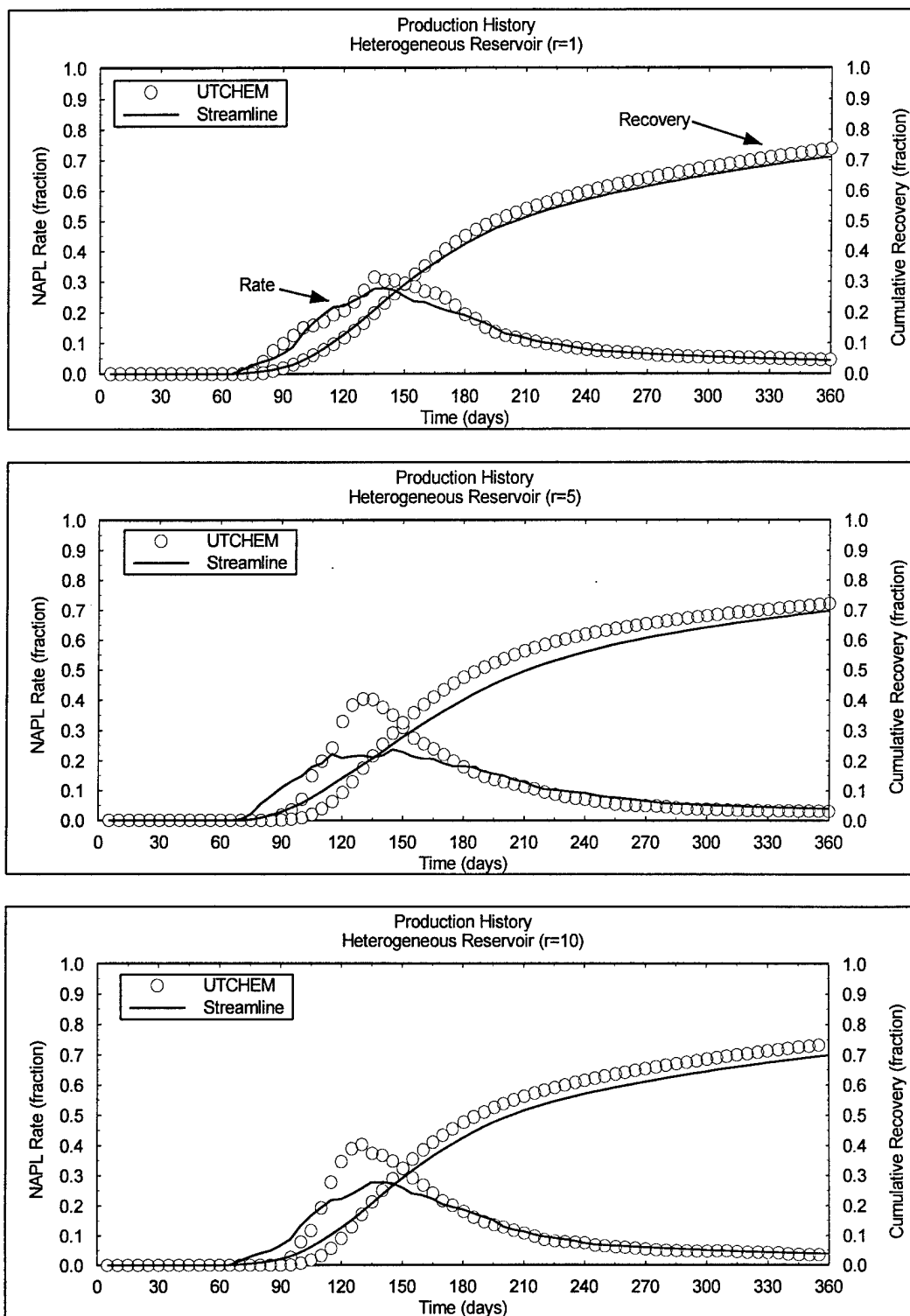
Fig. 8 – Effect of increasing correlation length of the permeability heterogeneity fields on production histories.

(see also **Fig.** 1). The lack of agreement between the streamline code and UTCHEM production rate histories at the longer correlation lengths may be due to the inability the streamline code to reproduce the interaction effects of the heterogeneity with the flooding. However, it is most likely that the streamline model can model the channeling effects better than UTCHEM. Note that the channeling effects were present in even the simplest water flood example discussed earlier. The streamline model assumes that the velocity fields remain constant throughout the duration of the simulation. Modification of the code so that the field is updated midway through the simulations might produce results that more closely resemble UTCHEM without a significant reduction in calculation efficiency. Additional testing of the streamline against field data is required to determine the accuracy of the predictions. The streamline code apparently "sees" the channeling more than the UTCHEM model because the streamline code shows an earlier breakthrough. However, the streamline models reproduces UTCHEM's prediction of the cumulative recovery history very well. Causes of these differences are as discussed previously.

Because the streamline model reproduces a production rate and recovery history most closely to that of UTCHEM with the shorter (more random) correlation permeability field, this field will be used for most of the future comparisons of performance. Limiting the permeability field to a
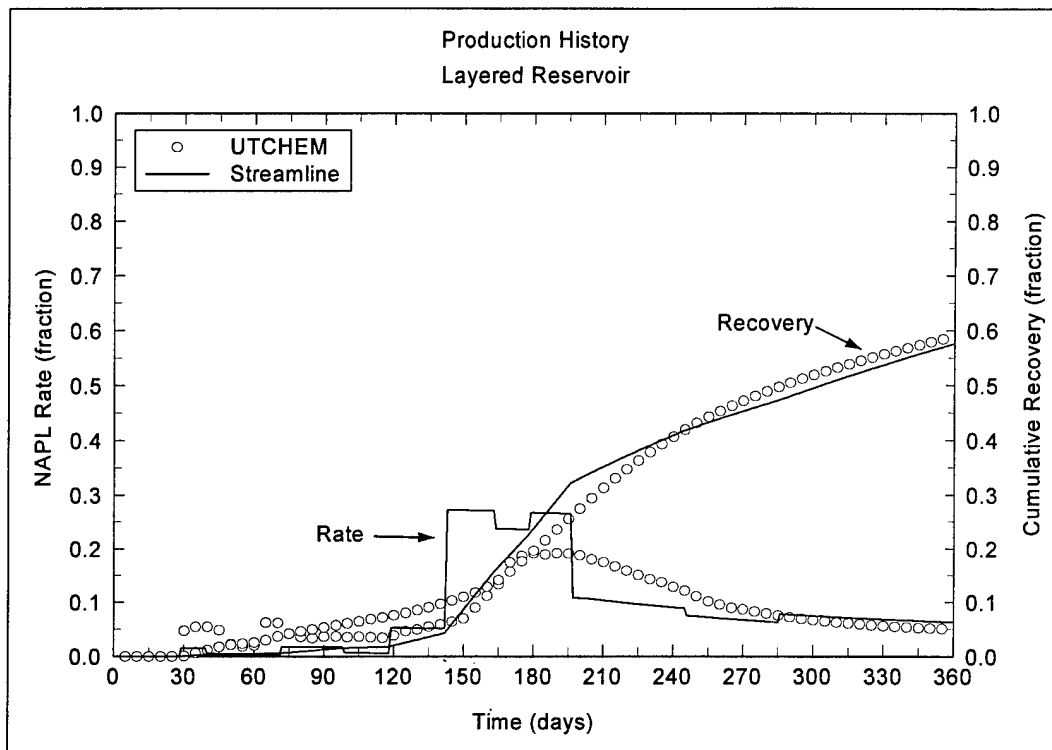
Fig. 9 – Production history of a layered aquifer.

short correlation length should not be a serious drawback, as the shorter correlation length is more representative of a typical aquifer. The streamline model is not limited to random permeability fields, as the following simulation demonstrates.

An extreme case of channeling is presented in **Fig. 9**, a production history for a simple layered aquifer. This permeability field has an average permeability of 1000 md with layers of high and low permeability randomly placed and varying between 100 md and 5000 md. The streamline code reproduces the UTCHEM production rate and cumulative recovery histories

very well. The numerical dispersion in the UTCHEM finite difference model is manifested in the production rate history by the rounding off of the NAPL bank shoulders. Also present in the UTCHEM model is the effect of cross flow that is not present in the streamline simulations.

## Slug Size

The effect of the injected slug size is most important to the economics of SEAR. Given a fixed quantity surfactant, it is often important to ask if the efficiency of the operation can be increased by increasing the surfactant concentration but injecting for a shorter time, or some other combination that uses the same total amount of chemical. This question has been examined by Larson (1979) and Pope and Nelson (1978).[21] In fact, some care was exercised in setting up the simulations to assure that the injected slugs were identical. This required an estimate of the mass of absorbed surfactant. The mass of injected surfactant is

$$M_i = (Q_i t) C_s \rho_s \dotfill (54)$$

The mass of surfactant absorbed is

$$M_a = \left(\frac{1-\phi}{\phi}\right) a_s \rho_r (Q_i t) \left(\frac{1}{1000}\right) \dotfill (55)$$

where $a_s$ is the number milligrams of surfactant absorbed per gram of rock.
and $Q_i$ is the injection rate of surfactant solution. In the streamline model,
the surfactant retention, $D_s$, is defined in terms of the ratio of the quantity
of surfactant absorbed to that injected.

$$D_s = \left(\frac{1-\phi}{\phi}\right)\left(\frac{\rho_r a_s}{C_s \rho_s}\right)\left(\frac{1}{1000}\right) \dots\dots\dots\dots\dots (56)$$

The UTCHEM model takes a slightly different approach to the
definition of surfactant retention. This model follows the approach of Lake
(1989).[8] In this approach, they have defined the surfactant retention as

$$D_s = \left(\frac{1-\phi}{\phi}\right)\left(\frac{C_{3S}}{C_s \rho_s}\right) \dots\dots\dots\dots\dots (57)$$

where

$$C_{3S} = \frac{a_3 C_s}{1 + b_3 C_s} \dots\dots\dots\dots\dots (58)$$

where $a_3 / b_3$ is the maximum absorption value. Although $a_3$ and $b_3$ are
functions of salinity, for a given concentration, the absorption can be treated
essentially as constant.[8] For the simulations of this study, a conservative
estimate of 0.04 was used for the streamline model absorption parameter.
Some attempts were made to determine the sensitivity of the streamline
code to the value of surfactant retention. For all reasonable values of $D_s$,

the effect of changing this parameter had little effect on the efficiency of the remediation. The model is much more sensitive to the effects of mobilization and solubilization of the NAPL. The fractional flow model relies heavily on the difference between the high tension and low tension fractional flow curves to determine NAPL production rates and times. The value of $D_s$ is typically on the order of 0.01. Changing the value of $D_s$ over the entire range of possible values will have little effect on the point of intersection on the high tension flow curve, which defines the NAPL bank saturation. An inspection of the graphical solution method used by the streamline model (**Fig. 3**) highlights why the value of the surfactant absorption has only a marginal effect on the overall recovery.

The slug size of the injected chemical is estimated as

$$V_{ps} = \frac{Q_i t C_s}{(A \cdot W)\phi} \quad \text{.............................................................................(59)}$$

where $A \cdot W$ is the volume of the aquifer. All of the simulations run with both the streamline model and UTCHEM used the same value of 0.076 for $V_{ps}$. The ratio of the slug size injected to the surfactant absorption ($V_{ps} / D_s$) is often used as a optimization guide for designing surfactant floods.[10] The ratio for the simulations of this study is 1.9, slightly high by enhanced oil standards but not unreasonable.

The effect of slug size on the recovery efficiency is a function of phase behavior and can become complex.[21] However, the effect of slug size on recovery efficiency was investigated with the streamline model and compared to that predicted by UTCHEM for a short correlation length permeability field (heterogeneous aquifer) with no added polymer.

The total amount of injected chemical ($V_{ps}$) was kept constant by doubling the injection rate and halving the injection time. Thus the effective chemical concentration was increased during the injection period from 4% to 8%. **Fig. 10** shows that both the streamline model and UTCHEM predict an
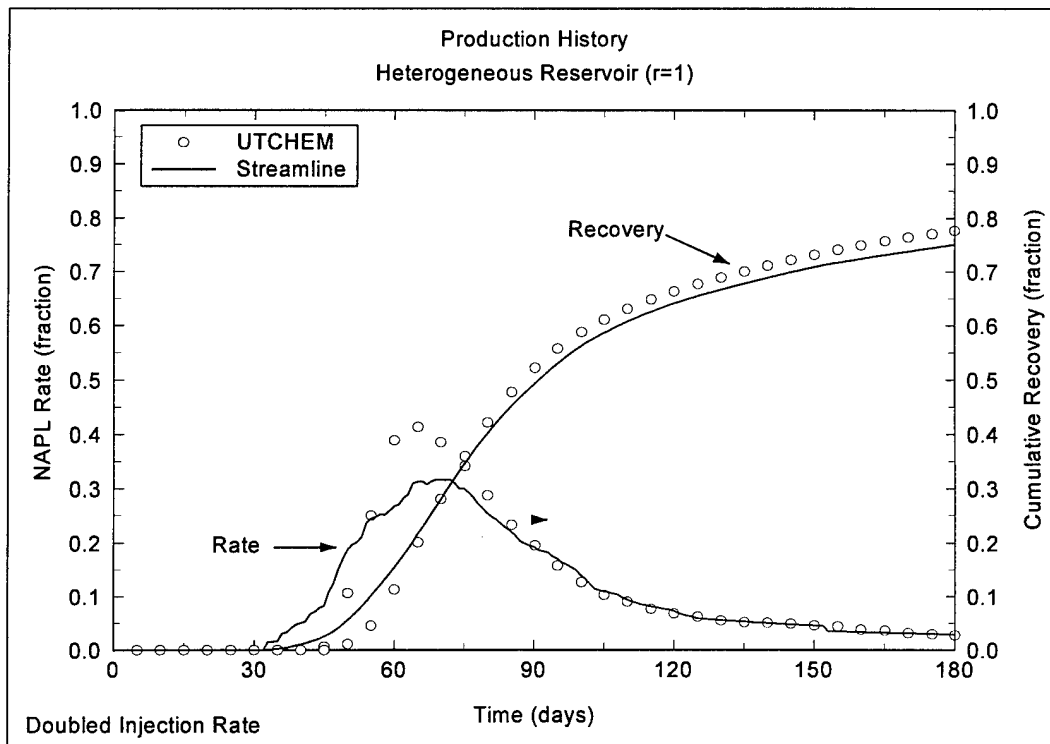


Fig. 10 – Effect of surfactant concentration with constant total surfactant injection ($V_{ps}$).

improvement in efficiency using this methodology. Note that not only do both UTCHEM and the streamline model predict an increase in efficiency (compare to **Fig. 8**), but the predictions of both models are almost identical. The cumulative recovery exceeds that in the lower concentration case, but it is exceeded after only 180 days of injection. Normally, in a SEAR application, the aquifer would continue to be flushed with water until all of the residual surfactant (and polymer, if any) is removed. This continued injection would remove NAPL throughout the time of the project until either all of the NAPL was removed or the residual saturation is reached.

## Residual Saturation

No doubt the residual saturation of the NAPL after a remediation project is one of the primary questions to be answered. The regulatory requirements for residual saturation of NAPL contaminants is orders of magnitude below that economically feasible for enhanced oil recovery and of critical importance to measure the success of a remediation project. Initial testing of SEAR, both using the finite difference simulator and in the field show promising results. The ability of any simulator to predict residual concentration and distribution of NAPL's is critical in the use of that simulator in the design of field applications.

Predicting residual saturations using fractional flow theory is difficult, primarily because of the complex phase behavior that occurs. The following simulations were made with the streamline model using only a first order approximation that the saturation of the NAPL phase is reduced beyond the initial reduction by mobilization caused by reduced IFT by the surfactant solubilization in the "tail" of the NAPL bank. This approximation makes use of the partition coefficient, which is an input parameter. Since all of the previous simulations occur in the Type II(–) region, the partition coefficient was kept low (between .01 and .05). The match between the UTCHEM model and the streamline model was achieved, as in the previous simulations, by adjusting the low tension relative permeability curves and the partition coefficient used by the streamline model. This adjustment allows the fractional flow model to capture the effects of solubilization and mobilization.

**Fig. 11** is a contour map of residual NAPL saturation resulting from a 365 day SEAR event in a homogeneous aquifer. Obviously, the general shape of the profile is consistent between the models. Most notable is the difficulty that the streamline model has in predicting the beginning of zero saturation levels. The UTCHEM simulation shows an optimistic (relative to the streamline model) minimum saturation that starts at an earlier time.
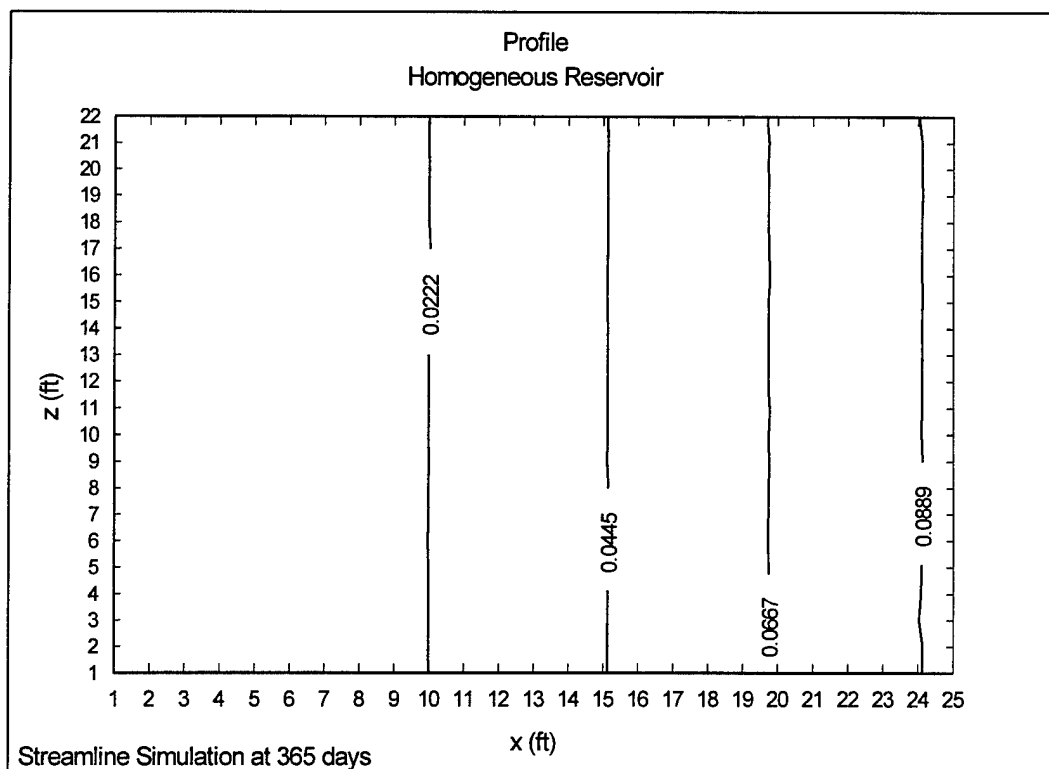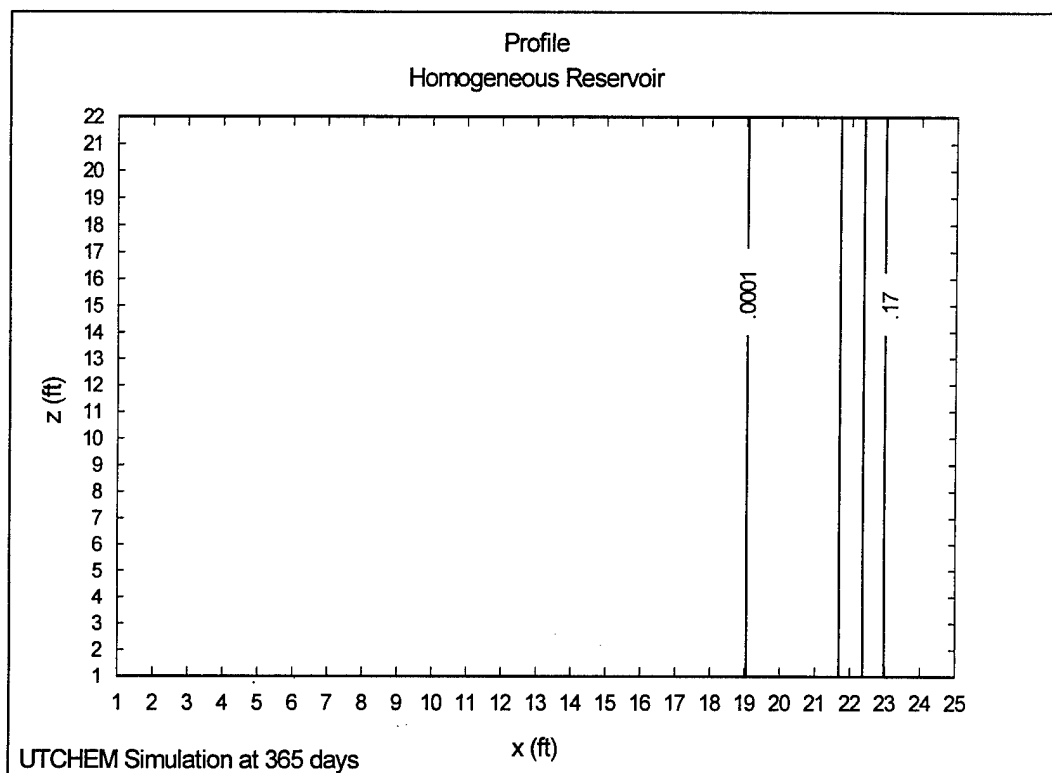
Fig. 11 – Homogeneous aquifer residual NAPL saturation profile.

The earlier starting time and later ending time is explained by an examination of the production histories for a homogeneous aquifer (**Fig. 7**). The numerical dispersion in the UTCHEM model tends to spread out the NAPL bank, so removal begins a little earlier and ends a little later. There is a strong possibility that UTCHEM model predicts greater cleanup because of the ability to model the phase behavior more exactly. However, the agreement is good (and an error slightly conservative is better than slightly optimistic in a remediation project). Moreover, as shown in the following examples, the agreement between the two models improves when heterogeneity is included in the simulation.

**Fig. 12** is a contour map of residual saturations in a short correlation length (r=1) heterogeneous permeability field for both UTCHEM and the streamline code. Again, the general shape of the two model's profiles are similar, showing the same location of low and high regions of saturation that is a result of the heterogeneity. The UTCHEM model shows the smoothing effect of the numerical dispersion in both the distribution of the contour lines and the beginning and ending times of the NAPL bank production. The streamline model has captured the essential effects of the heterogeneity. Both models are in agreement in the minimum predicted saturations (0.0001), though UTCHEM is more optimistic than streamline in the extent of this low saturation. Although, as with the homogeneous
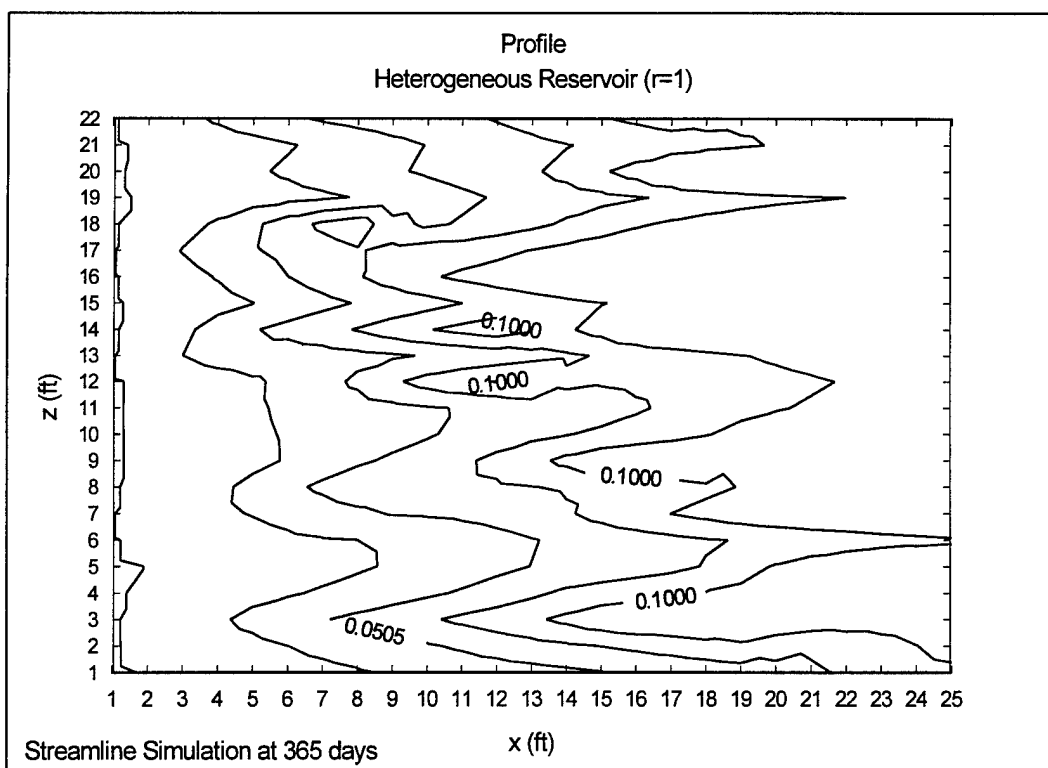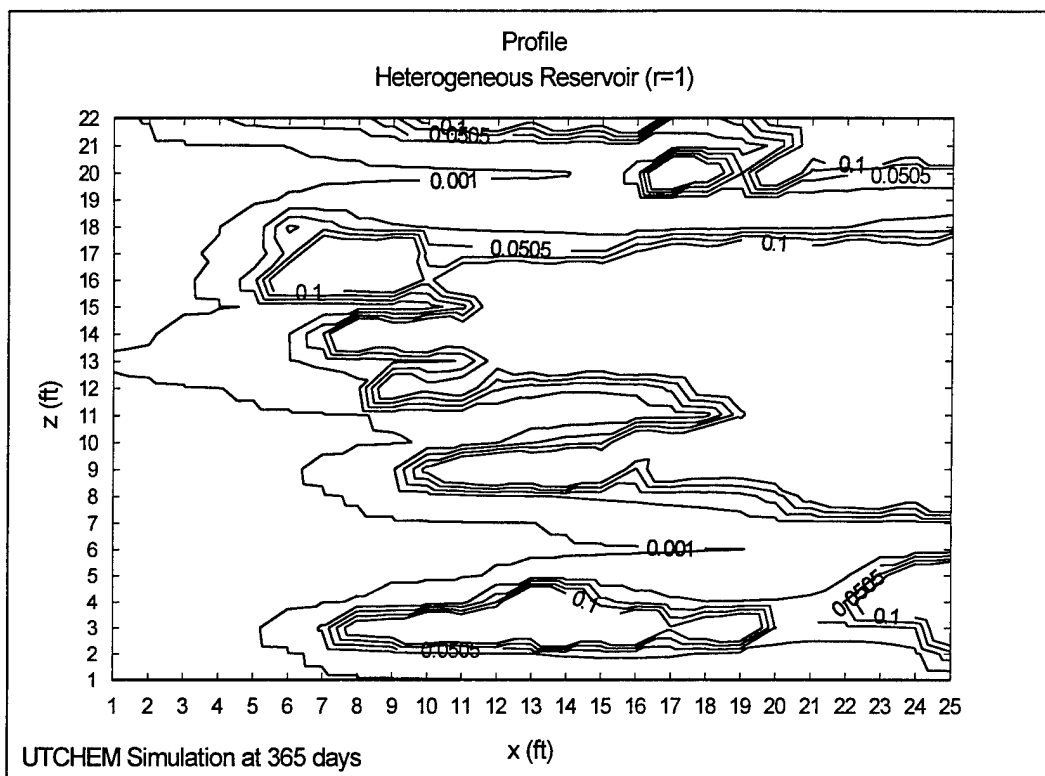
Fig. 12 – Heterogeneous aquifer (r=1) residual NAPL saturation.

aquifer, some of this is explained by the numerical dispersion (especially the lower saturations at the producer), probably a good deal of the differences are due to the ability of UTCHEM to reproduce the phase behavior and partitioning between the phases in more detail than the streamline code is currently capable. The inability of the streamline code to model interaction between the heterogeneity and the flooding is also a possible explanation for the differences as is the assumption of a constant velocity field that the streamline model makes.

**Fig. 13** is from a simulation that is similar in all regards to the previous examples except the random permeability field has a longer correlation length. In this case, the correlation length is 5 ft. (20% of the aquifer length) and the increased channeling effects are apparent over the essentially uncorrelated field previously shown (r = 1 ft.).

The contour maps of residual NAPL saturation in this example are more similar to each other than the two previous example. It appears that the streamline model is better at matching profiles of UTCHEM simulations in the more correlated aquifers than it is at reproducing production histories. Note that the location of the channels and general shape of the two profiles match very closely. There is some divergence in the residual saturations predicted, though not a great deal at the minimum. For example, both models predict a residual saturation of 0.0001 near the
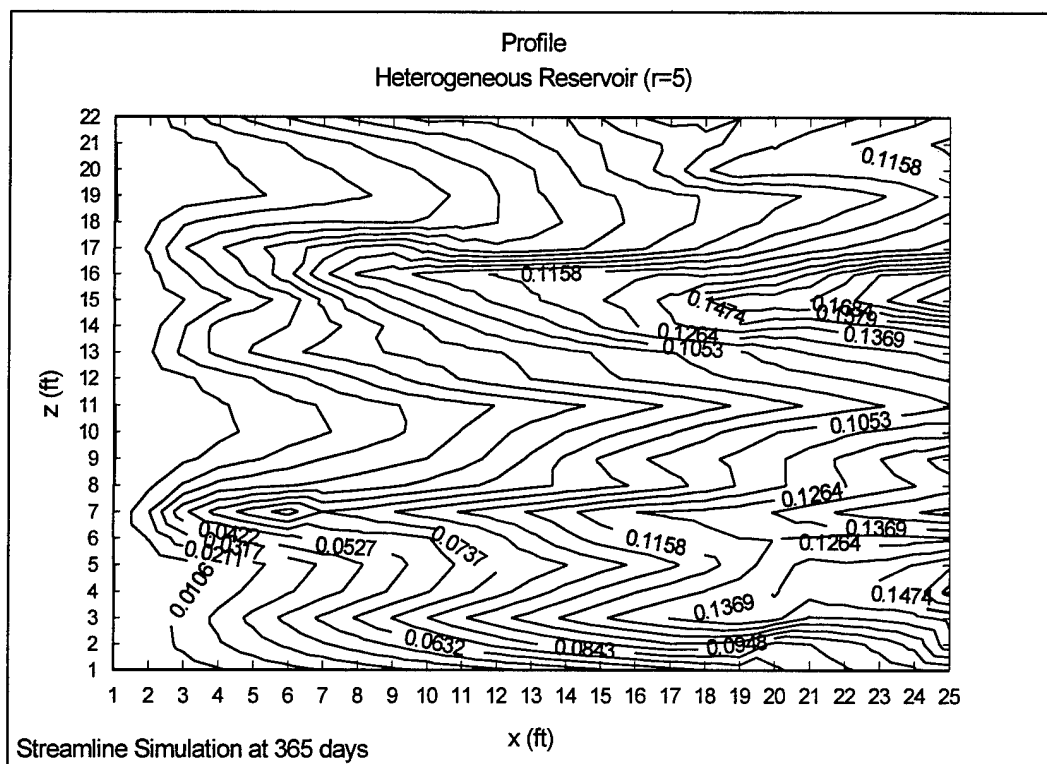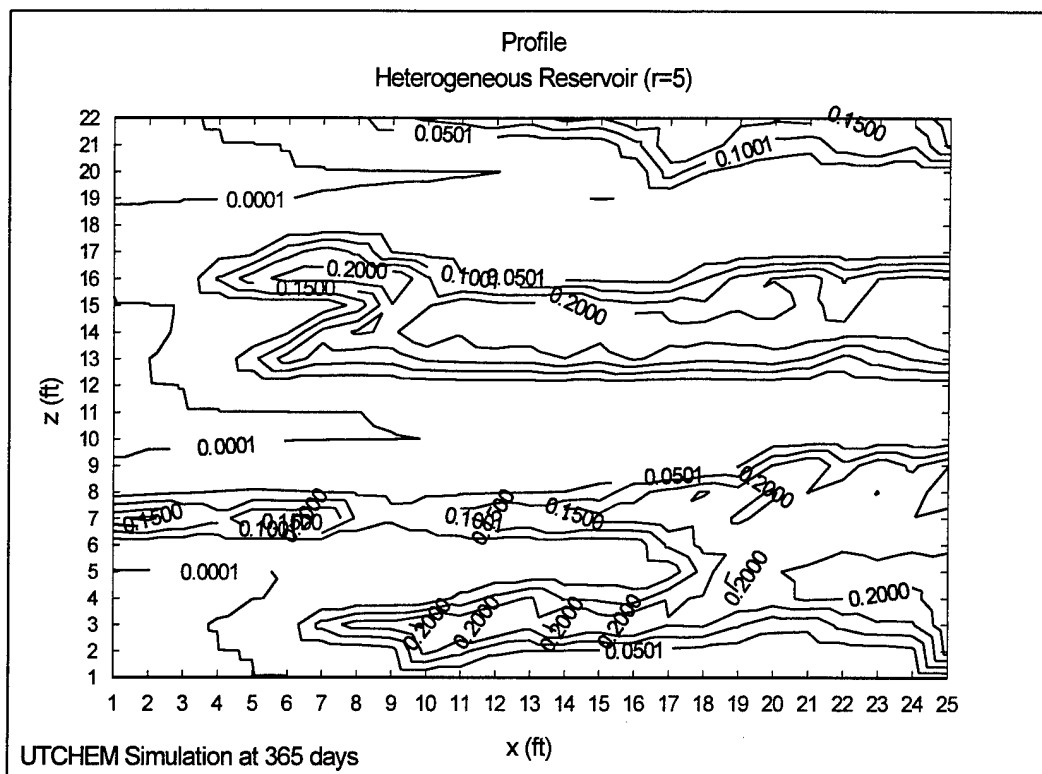
Fig. 13 — Heterogeneous aquifer (r=5) residual NAPL saturation.

injection well after 365 days of injection. Again, the UTCHEM simulator is more optimistic at the extent of the minimum saturations and less optimistic than the streamline model at the overall or aquifer average saturations. The streamline model is predicting a maximum saturation for the aquifer of 0.15 in pockets near the producer, while UTCHEM is predicting a maximum of 0.2 near the producer. Nevertheless, the agreement is quite good, considering the simplifications (not to mention time savings) of the streamline model.

**Fig. 14** is a contour map of the random permeability field with the longest correlation length (10 ft.). Both the UTCHEM simulation and the streamline simulation produce very similar profiles. This particular permeability field, with its long correlation length, demonstrates the greatest channeling effects. Note that the location of saturation contours are similar to the permeability contours in **Fig. 1**. Note also that the streamline model predicts saturation profiles better than production histories when modeling a highly correlated aquifer.

Both models predict that the minimum saturation after 365 days of saturation is 0.0001 near the injection well. UTCHEM is more optimistic in predicting the extent of the NAPL removal. Note that the contour for 0.001 saturation extends almost to the producing well in the UTCHEM profile. This trend is even more pronounced than the previous simulation. The
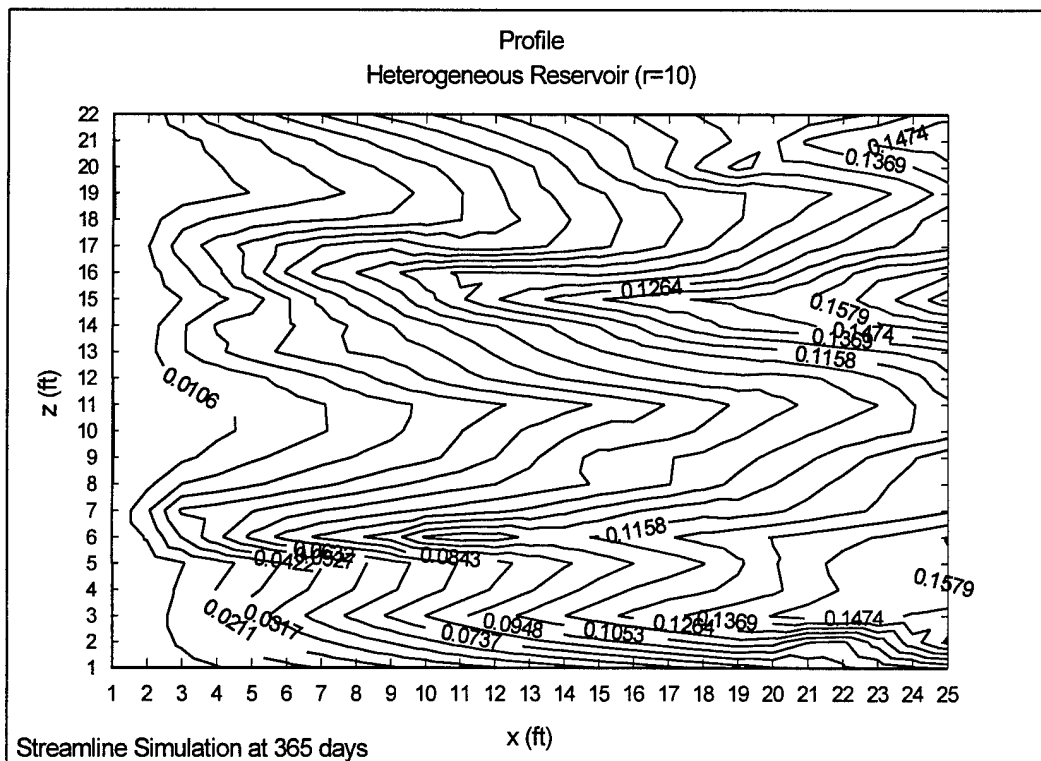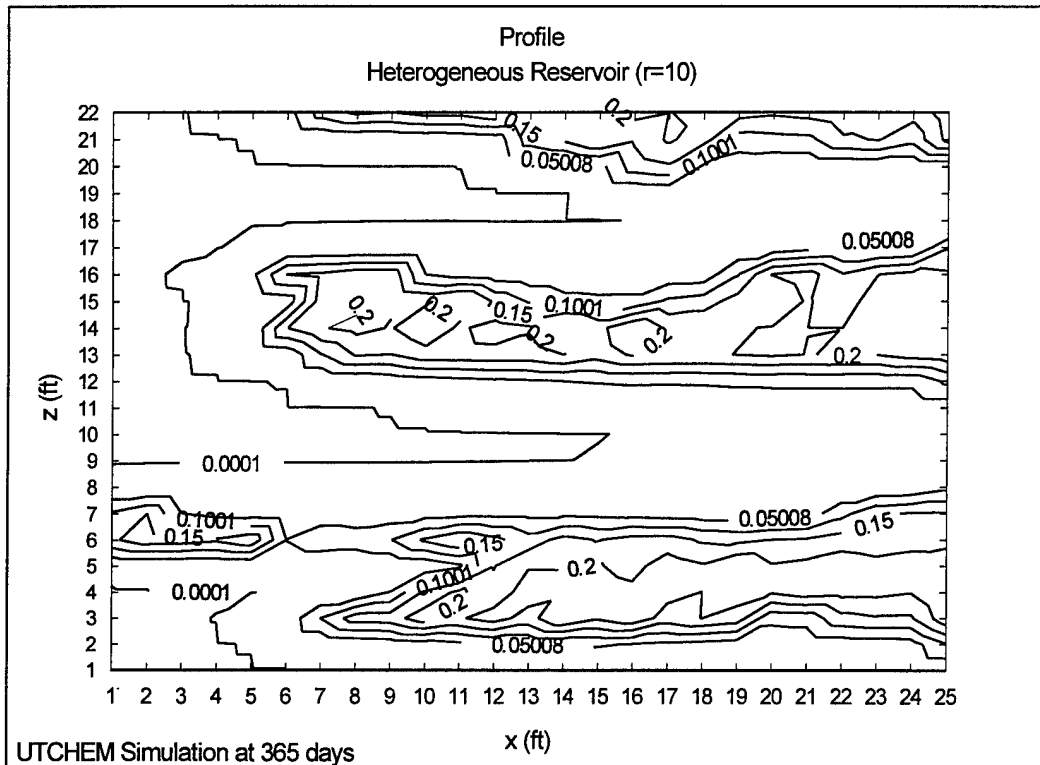
Profile
Heterogeneous Reservoir (r=10)

UTCHEM Simulation at 365 days

Profile
Heterogeneous Reservoir (r=10)

Streamline Simulation at 365 days

Fig. 14 – Heterogeneous aquifer (r=10) residual NAPL saturation.

streamline maximum saturation values are in very close agreement with UTCHEM. streamline predicts about 0.16 residual saturation near the producing well and UTCHEM about 0.15. UTCHEM predicts pockets of NAPL at the initial residual saturation value of 0.2. These pockets are not "seen" by the streamline model. The difference is probably explained as for the previous simulations: a combination of the way the streamline models the heterogeneity and flood interaction, the constant velocity field and the ability of UTCHEM to model the dynamic partitioning between phases.

The final simulation residual saturation contour map is presented in **Fig. 15**. This simulation is for the layered aquifer previously discussed. In this extreme correlation length aquifer, the effects of numerical dispersion that UTCHEM imposes becomes more obvious. The agreement between the two models is not as good as the previous examples. The location and shape of the residual NAPL saturation profiles produced by both models are quite similar. The minimum and maximum saturations predicted by both models agree as well as the previous random permeability fields. However, the saturations are much more spread out in the streamline produced profiles.

The maximum saturation predicted by both models is 0.2 and the minimum saturation is 0.0001. UTCHEM predicts an optimistic recovery. The extent of the lowest saturation value is larger than that predicted by the streamline model. In the layered aquifer model, the pockets of NAPL at
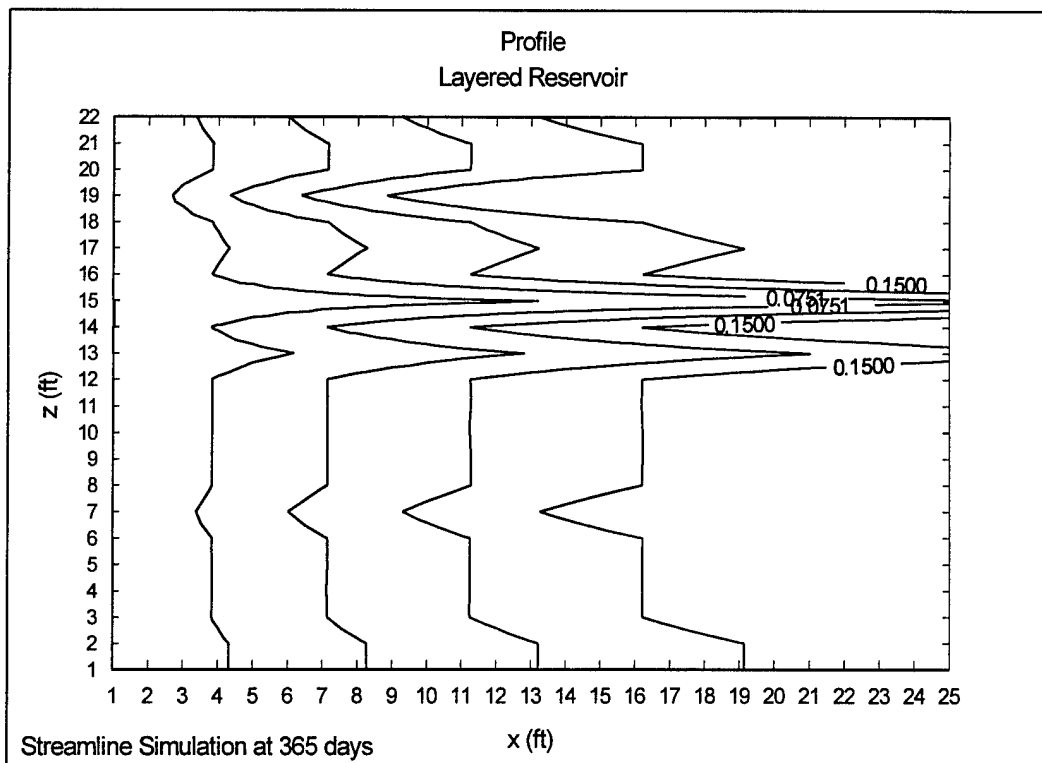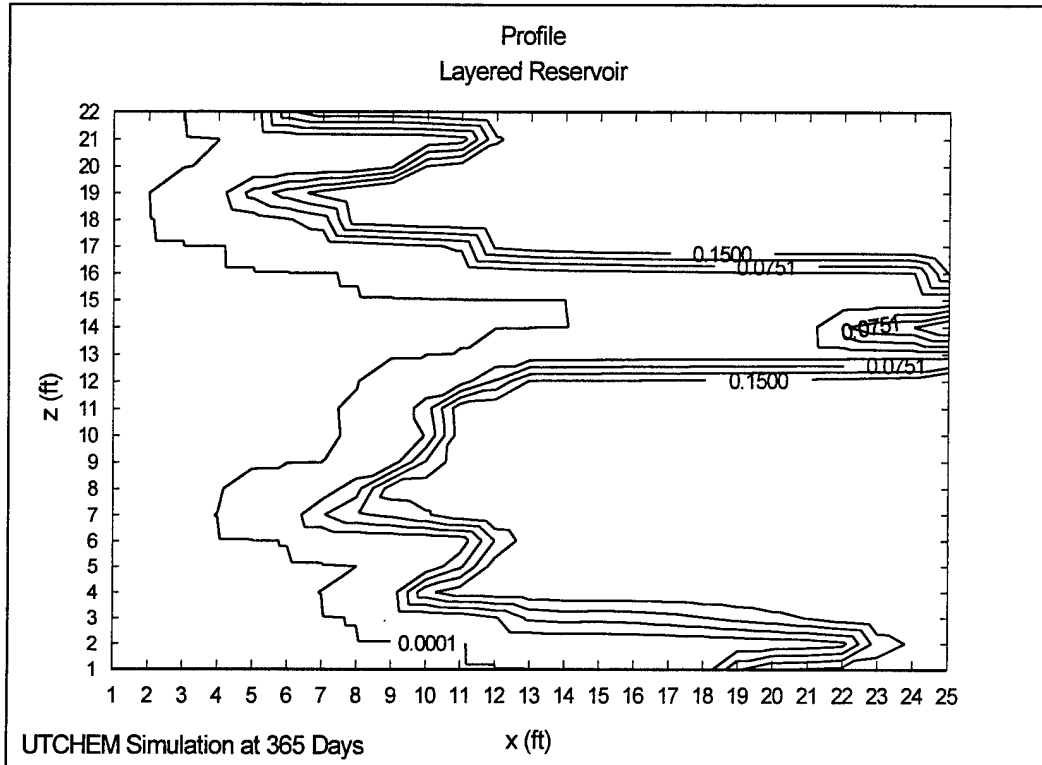
Fig. 15 – Layered aquifer residual NAPL saturation profiles.

the original saturation have disappeared. The agreement between the two models has increased, probably because there is less opportunity for the interaction of the heterogeneity and the flooding to become a factor in the simulation.

The streamline model appears to capture the effects of aquifer heterogeneity on residual saturation profiles nearly as well as the high resolution finite difference simulator. In fact, the streamline model behaves best in capturing residual NAPL saturation profiles when there is some heterogeneity. Note that the profiles predicted by the streamline model match those of UTCHEM worst for the homogeneous aquifer (see also **Fig. 11**). As important, the streamline model is less optimistic than UTCHEM in predicting the minimum NAPL saturation. This is useful in designing remediation projects as long as the model is not unreasonably pessimistic, which appears to be the case for these simulations.

## Solubilization and Mobilization

The effects of solubilization and mobilization are implemented in the streamline code by adjusting the partition coefficient and the low tension relative permeability curves to fit the known properties of the aquifer or to match the known production history. The mobilization of NAPL by the surfactant is captured by the effect of changing the shape of the low tension

relative permeability curves. The effects of solubilization are captured (at least a first order approximation) by the value of the partition coefficient.

Of the two mechanisms, the mobilization of NAPL is the more efficient in recovering NAPL contaminants from porous media. The mobilization of the NAPL occurs because of the reduction of the IFT between the phases that occurs with the presence of a surfactant. Abriola, *et al.* (1995)[9] has shown reductions in IFT to 0.09 dynes/cm in laboratory studies. The effect of mobilization on NAPLs is not always preferable. The reduction in the IFT between the phases may tend to allow downward movement through aquifer layers that were once acting as aquitards. The chances of the NAPL finding a vertical pathway (fracture, etc.) is enhanced when there is surfactant present. Fountain, *et al.* (1995)[7] recommends that to reduce the chances of vertical migration, a surfactant is selected that reduces the IFT by 1 order of magnitude or less. The effect of the surfactant on the low tension relative permeability curves is not well understood. Reference (8) contains a good discussion on the effects of surfactant on the low tension permeability curves.

The UTCHEM simulator uses many of the ideas in reference (8) to model the surfactant interaction with the NAPL. The streamline model simplifies the interaction to a simple change in relative permeability end points and exponent. Although the streamline model may miss some of the

finer details of solubilization, the results presented earlier show that the major effects are captured effectively. The simulation parameters were selected so that the entire SEAR process remained in a Type II(–) region where the effects are primarily limited to mobilization. Since the streamline code and UTCHEM do not model the low tension cases in the same way, some minor adjustment of the low tension exponent were some times required to obtain a good history match between the two models. The adjustment rarely exceeded 25%, however.

Since the exact effects of surfactant on the low tension permeability is
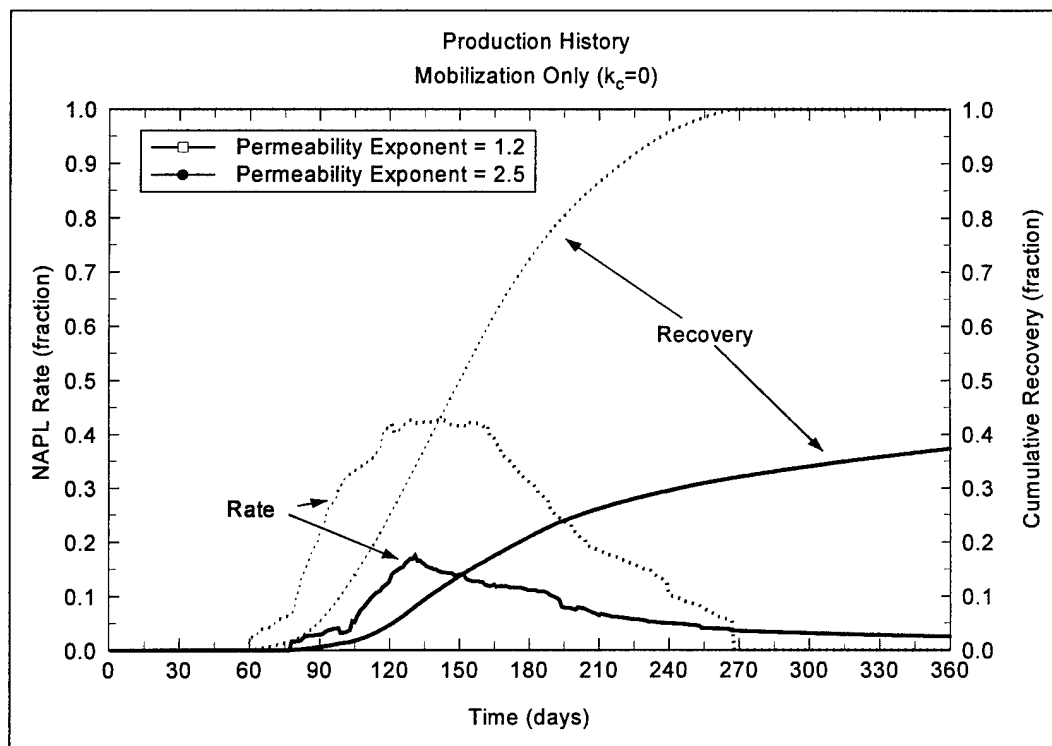


Fig. 16 – Effect of changes in relative permeability curve exponents, mobilization only.

not well understood, this minor difference is acceptable. The advantage to the considerable ease in programming in the streamline model is countered only by the requirement for more user interaction with the code in adjusting the low tension permeability curves to obtain a good history match.

**Fig. 16** demonstrates the effect of changing the relative permeability exponents on the production history when only mobilization is present. For these simulations, the partition coefficient, $k_c$, is set to zero and the relative permeability exponents are changed. Both simulations in the graph are from the streamline model. The solid line represents the rate and recovery histories when there is low mobilization. The dashed line represents the same histories when the mobilization effect is high. Note that a small change in the effect on the relative permeability exponents has a dramatic effect on the cumulative recovery. Clearly, the mobilization is important and small adjustments to the input parameters can have a large impact on the production histories.

The effects of solubilization on the SEAR process are much more complicated than those of mobilization. Abriola, *et al.* (1995)[9] and Pennell, *et al.* (1993)[2] have reported the results of laboratory investigations on NAPL solubilization by surfactant. The effect of solubilization appears to be rate limited and any SEAR process requires attention to length of contact time of the surfactant with the NAPL to estimate the effectiveness of the

remediation.[9] A good model does not currently exist that captures all of the effects of the mass transfer.

The streamline code implements the effect through the partitioning coefficient ($k_c$) as suggested by Larson (1979).[21] An essential assumption in this model is that the reactions are fast enough compared to the fluid flow so that a chemical equilibrium exists at all times and that there are no chemical reactions that occur. As mentioned previously, this is not always true. The UTCHEM model does include some of the possible chemical reactions and thus makes comparing results of the two simulators difficult
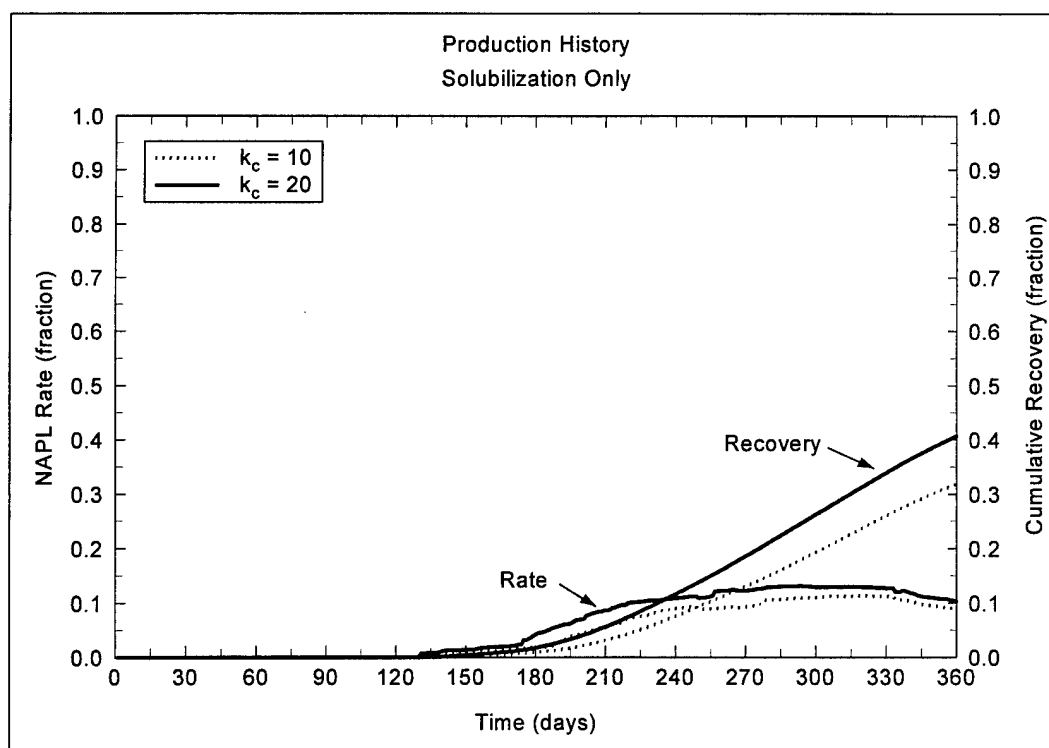


Fig. 17 – Effect of changes in the partition coefficient, solubilization only.

when the SEAR process is in the type (III) or type II(+) regions where solubilization is an essential part of the remediation process. Note from previous simulations, though, that the simple addition of a constant partition coefficient is adequate for many cases.

**Fig. 17** is the production histories from two streamline simulations where there is only solubilization of the NAPL phase occurring. This was accomplished by letting the permeability exponents remain essentially the same for both the high and low tension situation and varying the partition coefficient. The two simulations presented use $k_c = 10$ and $k_c = 20$. Note that not only is solubilization less important than mobilization, but also that increasing the solubilization has less impact than changes in the relative permeability curves. The effect of the solubility occurs later in the production history. This is because in the fractional flow model, the solubilization occurs only in the "tail", after the NAPL bank saturation has passed. With the streamline model, it is very important that the value of the partition coefficient be chosen carefully. It is possible to create unrealistic production histories, because the code is not able to distinguish valid values of the coefficient. For example, replacing $k_c = 10$ with $k_c = 5$ will predict 100% recovery at 180 days in the previous example.

## 3-D Simulation

The ultimate test of the streamline simulator is it's ability to estimate production histories an residual saturations from large, three dimensional aquifer models. For this simulation, a three dimensional random permeability field was generated using GSLIB, assuming a 1 ft. correlation length. The dimensions selected were 20 blocks x 20 blocks x 10 blocks (x, y, z), each block 10 ft. on a side. Total dimensions of the aquifer are 4000 blocks, 200 ft. x 200 ft. x 100 ft. All other aquifer parameters are unchanged from the previous simulations. Due to memory constraints, both the streamline and UTCHEM simulations were run on a SPARC workstation, rather than a desktop PC.

**Fig. 18** is the production rate and cumulative recovery histories from both the UTCHEM and streamline models for the 3-D heterogeneous aquifer described above. The difference in the histories is more pronounced than that of the 2-D aquifer used for most of the simulations. Although the shape of the production rate history is not very close, there is reasonable agreement between the cumulative production histories. Moreover, the cumulative production history seems to be converging between the two models at longer times. The inability of the streamline model to reproduce the predictions of UTCHEM are more pronounced for 3-D simulations.
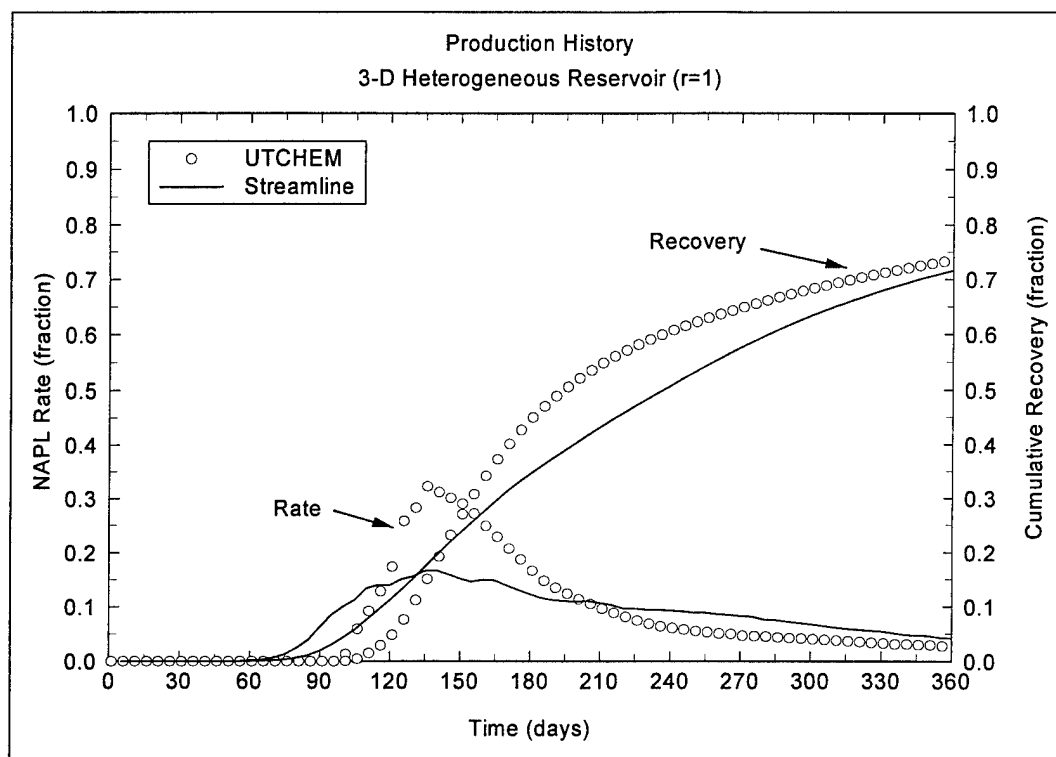
Fig. 18 – Production histories for a 3-D aquifer.

## Simulation Time

One of the greatest advantages that the streamline model has over a finite difference model is the reduction in simulation time. The ability of the streamline code to closely capture all of the effects of a surfactant flood at least an order of magnitude faster than the finite difference model makes it a good candidate to design and model SEAR processes in the field at least in the initial phases. To test the ability of both codes to run on a variety of platforms, the source code was compiled on several different computers.

| TABLE 2 – COMPUTERS USED IN SIMULATIONS | | | |
|---|---|---|---|
| Computer | Laptop PC | Desktop PC | SPARC Workstation |
| CPU | 486DX2 50Mhz | Pentium 83Mhz | 4 Ross Processors |
| RAM | 8Mb | 24Mb | 256 Mb |

**Table 2** summarizes the characteristics of each computer on which the simulations were run.

The differences in time required to complete a 365 day simulation are striking. **Table 3** summarizes the times required for the various simulations discussed previously. There are several noteworthy items from this summary. First, the streamline simulator is at least 60 times faster than UTCHEM for a homogeneous aquifer and at least 250 times faster than for a heterogeneous aquifer, running on PC. When the size of the aquifer increases in the number of gridblocks (and dimensions) the difference between the two model's simulation times becomes even greater. The size of the array prevents the models to run on a PC, so the 4000 grid block simulation was conducted on the SPARC workstation. For the large array, the streamline simulator was about 60 times faster than UTCHEM. Though the relative difference in time required to complete a simulation is only an order of magnitude faster, the absolute time required to run the simulation makes it very inconvenient if not impractical for use in designing or studying field applications. The cost alone of the computer time for

| TABLE 3 – TIME REQUIRED FOR VARIOUS 365 DAY SIMULATIONS | | | | | | |
|---|---|---|---|---|---|---|
| | Laptop PC | | Desktop PC | | Workstation | |
| | Stream | UTCHEM | Stream | UTCHEM | Stream | UTCHEM |
| 550 Grid Block Homogeneous | 10 secs. | 15 min. | 3.5 secs. | 5 min. | 10 sec. | 20 min. |
| 550 Grid Block Heterogeneous | 10 secs. | 49 min. | 3.5 secs. | 15 min. | 10 sec. | 58 min. |
| 4000 Grid Block Heterogeneous | N/A | N/A | N/A | N/A | 50 secs | 51 hrs |

UTCHEM may sometimes prohibit its use. Since UTCHEM is essentially a IMPES reservoir simulator, very small time steps are required to prevent instabilities in the output or causing the program to crash.

The streamline model seems limited only by the available memory to the computer. Not included in the above table, because the simulation was not repeated for all of the computers, was a 2000 grid block heterogeneous aquifer simulation on the desktop PC. The time required for this simulation was only 7.5 seconds. There was insufficient memory available for the laptop to run either the UTCHEM or the streamline model and there was insufficient memory available to run the UTCHEM model on the desktop. Note that the relative times required to run either code on any machine are about the same. Most probably, the addition of memory to the desktop machine would allow it to run very large arrays very quickly at very low cost. Moreover, the streamline model was very robust. The size of the time step is very unimportant in the time required for the simulation or the

quality of the output. The streamline simulations of this study were all conducted with a one day and five day time step. There was no discernible difference in the output time or quality of the output using either timestep.

## Dispersion Effect in UTCHEM

Although the effects of longitudinal and transverse dispersion was not included in the streamline simulation study, several simulations were run in UTCHEM to see how changes effect the recovery rate and cumulative recovery histories.

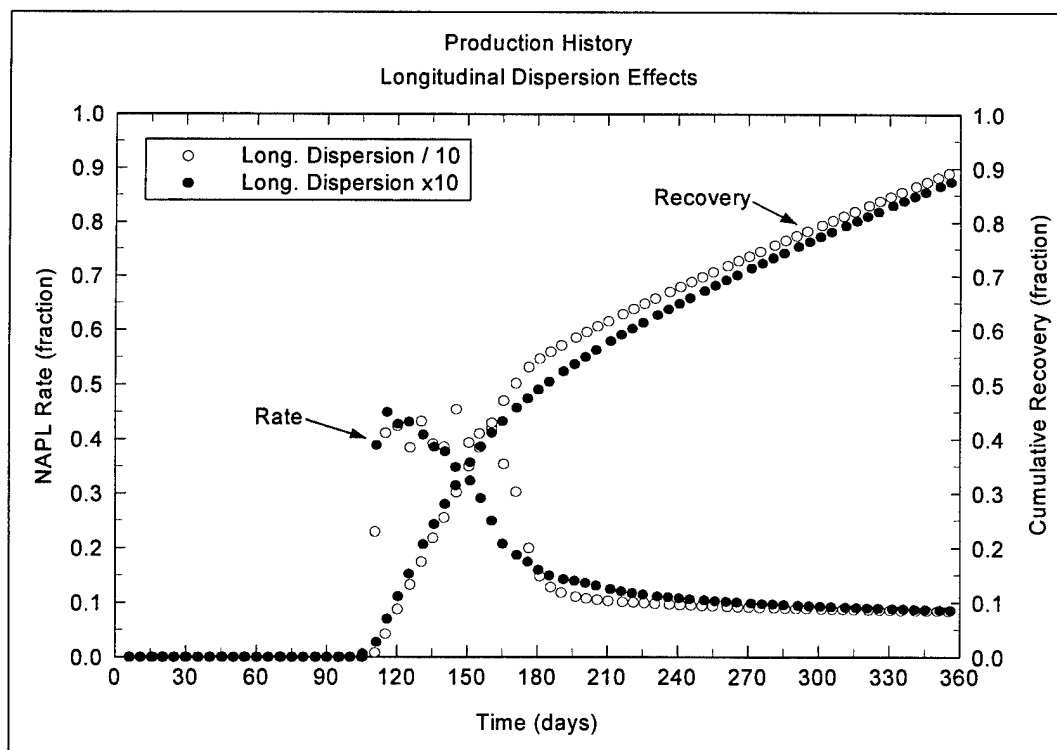**Fig. 19** shows the effects of changing the longitudinal dispersivity by



Fig. 19 – Effect of longitudinal dispersion, UTCHEM.

two orders of magnitude on a homogeneous aquifer. The longitudinal dispersion was increased upward by a factor of 10 over the base case parameter (compare to the base case in **Fig. 7**). The results are in the solid symbol. Note that the dispersivity had only minor effects on the shape of the production rate and virtually no change in the cumulative recovery (perhaps a small decrease). Decreasing the longitudinal dispersivity by a factor of 10 "sharpened" the tail of the NAPL bank slightly and did not change the cumulative recovery relative to the base case.

**Fig. 20** shows the effects of changing the transverse dispersivity by 2 orders of magnitude on the same homogeneous aquifer as above. The effect of transverse dispersivity is essentially unnoticeable for these studies. The two production curves overlay each other exactly on the scale presented in **Fig. 20**. This is not unexpected, given the fairly low dispersivity assumed for the base case and the 10:1 anisotropy ratio in the z direction. The very low effect of dispersivity on the production histories confirms that, for these studies, leaving dispersion effects out of the streamline simulations do not have a significant impact on the reported results. It is also apparent that the effects of dispersion leading to differences between the streamline model and UTCHEM are more likely due to numerical dispersion than modeled dispersion. Note that decreasing the longitudinal dispersion by an order of magnitude had almost no effect on the output from UTCHEM. It is possible
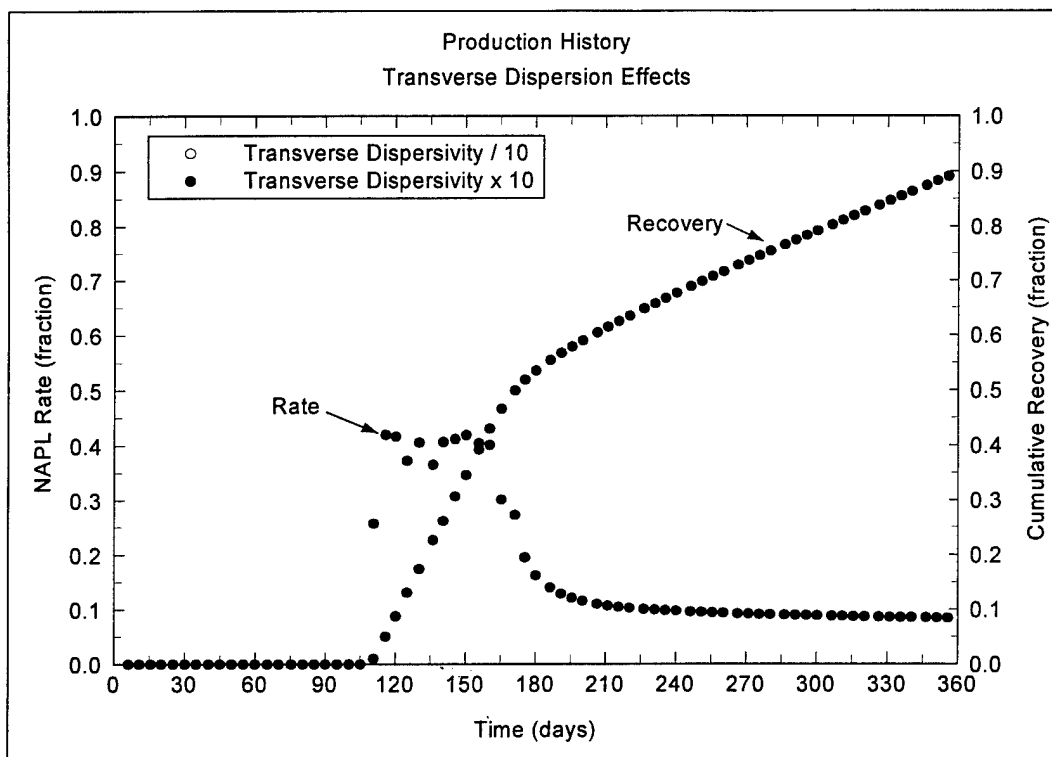
Fig. 20 – Effect of transverse dispersion, UTCHEM.

to include the effects of longitudinal dispersion in the streamline code, if there is a requirement for this effect to be studied.

# CHAPTER V

# SUMMARY AND CONCLUSIONS

## Summary

Surfactant Enhanced Aquifer Remediation is an area of heightened interest for groundwater management. The application of surfactant technology from enhanced oil recovery is showing promise in both laboratory and field investigations. The ability of surfactants to reduce the interfacial tension between the NAPL and the aqueous phases and its ability to solubilize NAPL and hold the solubilized oleic phase in suspension while it is transported through the aquifer makes it an ideal replacement to traditional "pump and treat" remediation schemes. These properties greatly enhance the efficiency of the SEAR process.

The field applications, though promising, have shown mixed results. The inability to make accurate predictions for a remediation process has focused the attention of many on modeling the process mathematically. These models are used to design computer programs that allow accurate and efficient testing of the effects of many different parameters that interact in the subsurface and can influence the outcome of the SEAR process. Modeling the interaction of all of the parameters in the subsurface has

proven to be difficult as well. The most successful model reported to date uses a finite difference simulator originally designed as an oil reservoir chemical flood simulation. This model, though it seems to predict field cases with reasonable accuracy, suffers from being very slow and prone to instabilities due to the finite difference design.

A streamline approach to modeling fluid flow through a porous medium, already an accepted method of modeling tracer flow through heterogeneous medium, can be extended to modeling two phase flow using fractional flow theory. Fractional flow theory for surfactant injection was applied to a streamline model and tested against an accepted finite difference simulator with excellent agreement. The new streamline model was capable of reproducing all of the major effects predicted by UTCHEM when changing a variety of different parameters. The streamline code made accurate predictions of production histories and residual saturation profiles of 2-D vertical cross sections and 3-D heterogeneous aquifers despite many simplifications that were assumed when designing the code.

The effects of mobilization of NAPL by an injected surfactant was assumed to be contained only in the effect it had on the low tension relative permeability curves for NAPL and water. Minor adjustments to the model parameters for end-point saturations and exponents could reproduce almost exactly the production histories and profiles predicted by UTCHEM, even

though these parameters in the streamline code were assumed constant. This is a simplification that UTCHEM does not make.

The streamline model assumes that all of the effects of polymer addition to the injected stream are captured by the effects on the mobility by changing the viscosity of the injected stream. Even though the streamline code assumes that the viscosity is constant, (again, a simplification that UTCHEM does not make) it is capable of reproducing almost exactly the effects of the additional polymer on the production histories for the cases studied. The effect of the interaction of polymer with the surfactant and the aquifer salinity can become very complicated, however. The streamline model does not capture all of the phase behavior that occurs with an injected polymer.

The effects of solubilization are probably least accurately modeled in the streamline code, though currently there is no accepted "best" model. The streamline code assumes that the effects of solubilization can be captured through three constant input parameters, the most important of these being the partition coefficient for the partitioning of NAPL between the oleic phase and the aqueous phase. The streamline model was capable of capturing the effects of solubilization very well for the simulations of this study by minor adjustments of the partition coefficient. Even more extreme effects seem to be captured for very large partition coefficients, though the

phase behavior can become very complicated and the simplified code may not be capable of reproducing all of the details predicted by UTCHEM.

The combined effects of solubilization and mobilization are important to be understood. Because mobilization is so much more efficient at removing NAPL contaminants from an aquifer, it should be exploited as much as possible. However, there may be some instances where the enhanced mobilization of the may increase the downward spread of the NAPL through layers that were once impervious the NAPL because of the high interfacial tension. These include layers that were once aquitards because of their low porosity and fractures that were previously too small to allow the NAPL to flow through. If there is an opportunity for the NAPL to spread, then solubilization of the trapped NAPL may be the preferred alternative. Both UTCHEM and the streamline model predict the effects of solubilization and mobilization. Because of the simplifications that were required in developing the phase behavior of streamline, care must be exercised in choosing partition coefficients. It is possible to choose a partition coefficient that predicts unlikely production histories.

The forte of the streamline code is its ability to provide results very quickly, using modest computational power, despite complications of heterogeneity. Its speed is due to the fact that it need only to solve a finite difference equation once for any simulation in order to determine the

velocity field for the aquifer. Once this field is determined, transit times for streamlines are calculated. The number of streamlines is determined by the user and depends on the level of detail desired. The velocity field is assumed to remain constant, shown to be a reasonable approximation, though updating this field is possible and may provide more accurate results than the current code. Along the streamlines, tracer concentrations are calculated analytically. More importantly for two phase flow and the application of fractional flow theory, the fractional flow rate (and thus saturation) at a point is dependent only on the transit time to that point. This makes estimates of flow rates and saturations a simple analytical calculation of a one dimensional problem along each streamline.

The effects of these analytical methods are dramatic. The streamline model is capable of reproducing in seconds, almost identically, a simulation that with UTCHEM takes 15 minutes on a desktop PC. More striking is the ability of the streamline code to complete a simulation in seconds running on a typical laptop computer that requires an hour with UTCHEM running on the same laptop. The speed and robustness of the code follow through in 3-D simulations as well. Large numbers of grid blocks required for detailed studies of aquifer heterogeneities make finite difference simulations almost impossible. Simulations that take days with UTCHEM are made in seconds with the streamline model. The ability of the streamline code to produce

accurate results quickly are limited only by the amount of RAM available and not by the horsepower of the CPU.

## Conclusions

Surfactant enhanced aquifer remediation is a technology that is a promising alternative to traditional "pump and treat" remediation methods for contaminated groundwater. This technology is effective and efficient at removing unwanted NAPL contaminants from porous media.

Accurate and efficient mathematical models are required to predict the effects of injected surfactants in a subsurface porous medium. The inability of predicting the success of a remediation process from laboratory study is detrimental to using SEAR technology in a field application.

All of the effects of surfactant injection into a subsurface porous media are not understood. The complicated interaction of the flood with the heterogeneity and the unusual phase behavior that is sometimes seen makes prediction of results difficult.

Many of the mathematical models developed for the SEAR process are inadequate for a variety of reasons. Some do not consider heterogeneity, others are limited to one or two dimensions while others focus on only one aspect of the surfactant process, either mobilization or solubilization.

The most accurate model developed to date, UTCHEM, is too slow and unstable to be useful in designing applications of SEAR in the field. However, UTCHEM, because of its ability to predict almost all aspects of a surfactant flood, serves as an excellent benchmark to judge the performance of any other model.

Fractional flow theory is a simplified approach to modeling fluid flow through a porous medium. It can be adapted to model the effects of polymer and surfactant in the injected stream. These adaptions allow the fractional flow theory to be applied to the streamline model with relative ease. The complicated interactions are reduced to a simple, one dimensional calculation along a streamline.

The streamline model with fractional flow theory applied to model to model the behavior of two phase flow with partitioning between the phases accurately captures the effects of a surfactant flood in a NAPL remediation process for homogeneous and heterogeneous aquifers in one, two, and three dimensions.

The streamline model is orders of magnitude faster than the benchmark finite difference reservoir simulator. Simulations that require hours or days with UTCHEM are completed in seconds with the streamline model. Moreover, the streamline code is very robust, making selection of input parameters irrelevant to the output.

The streamline model is capable of running on modest desktop and laptop PCs, making it an excellent candidate for designing SEAR applications in the field. The size of the aquifer and the number of grid blocks desired is limited only on the memory available to the computer.

The effects of mobilization of the NAPL by the surfactant are captured accurately in fractional flow theory by the relative permeability model used and the parameters selected to model the low tension and high tension relative permeability curves.

The effects of solubilization of the NAPL by the surfactant are captured accurately by a partition coefficient that measures the relative amounts of NAPL that partitions between the oleic phase and aqueous phase. The partition coefficient can be assumed constant for most SEAR processes. The correct choice of a partition coefficient is important for the streamline model to predict the effects of solubilization.

The effect of adding polymer to a SEAR process is captured accurately by the effect of the polymer on the aqueous phase viscosity. The effect on the viscosity can be assumed constant for most SEAR processes.

Adding polymer to a SEAR process is desirable in that the efficiency is increased. More NAPL is recovered faster. Since polymer is generally less expensive than surfactant and very small amounts of polymer have

dramatic improvements on the SEAR process, it is economically more efficient as well.

The effect of mobilization and solubilization need to be studied carefully. Mobilization is more efficient at removing NAPL from an aquifer, so should be used if it is possible to do so without spreading the contaminant due to downward diffusion through fractures and aquitards.

Modification of the streamline code so that the velocity field may be updated more than once throughout the simulation should be investigated to determine if the predictions more closely match those of UTCHEM.

The effects of solubilization and polymer injection on the phase behavior of the surfactant flood should be investigated to determine if these effects should be modeled in the streamline code. If the effects are important, then the streamline model should be modified to include the behavior of the surfactant flood under greater polymer concentrations and higher salinities.

The streamline code should be tested against field results to measure how well the code models a "real" remediation process.

The streamline model developed for SEAR applications can be applied to standard enhanced oil recovery simulations with little modification while retaining all of the benefits of the streamline model mentioned previously.

# NOMENCLATURE

A    =    Area, ft$^2$

$\hat{C}_i$    =    Concentration of component i on the aquifer rock, fraction

$C_{ij}$    =    Concentration of component i in phase j, fraction

$D_s$    =    Surfactant adsorption, dimensionless

$N_p$    =    Oleic phase (NAPL) production, ft$^3$

$Q_i$    =    Injection rate, ft$^3$/sec

$S_j$    =    Saturation of phase j, fraction

$S_{obt}$    =    Oleic phase saturation at chemical breakthrough, fraction

$S_{or}$    =    Residual oleic phase (NAPL) saturation, fraction

$S_{orc}$    =    Oleic phase saturation with chemical (surfactant) present

$S_{wb}$    =    NAPL bank water saturation, fraction

$S_{wi}$    =    Initial water saturation, fraction


$f_{wb}$    =    Fraction flow of aqueous phase in NAPL bank, fraction

$f_{wi}$    =    Initial fractional flow of aqueous phase, fraction

k    =    Permeability, md

$k_c$    =    Partition coefficient, dimensionless

$k_o$    =    Ratio of the concentration of NAPL in the injected aqueous phase

to the concentration of NAPL in the equilibrium oleic phase

$k_{oo}$ = Concentration of the NAPL in equilibrium oleic phase

$k_r^0$ = Endpoint relative permeability, dimensionless

$k_{r\alpha}$ = Relative permeability, dimensionless

$p$ = Pressure, psia

$q_t$ = Volumetric flow rate, $\text{ft}^3/\text{sec}$

$r$ = Correlation length, ft

$t_D$ = Time, dimensionless

$v_{\Delta C_1}$ = Velocity across the aqueous phase shock front, ft/sec

$\psi$ = Stream function

$\omega$ = Stream function

$\chi$ = Stream function

$\mu$ = Viscosity, cp

$\phi$ = Porosity, fraction

$\lambda$ = Fluid mobility, dimensionless

# REFERENCES

1.  Wilson, J.L. and Conrad, S.H.: "Is Physical Displacement of Residual Hydrocarbons a Realistic Possibility in Aquifer Restoration?," *Proceedings of the NWWA Conference of Petroleum Hydrocarbons and Organic Chemicals in Groundwater: Prevention, Detection, and Restoration,* National Water Well Association, Dublin, OH (1984) 274–298.

2.  Pennell, K.D., Abriola, L.M., and Weber, W.J. Jr.: "Surfactant-Enhanced Solubilization of Residual Dodecane in Soil Columns," *Environ. Sci. Technol.* (1993) **27,** No. 12, 2332–40.

3.  Fountain, J.C.: "The Use of Surfactants for In-Situ Extraction of Organic Pollutants from a Contaminated Aquifer," *J. Hazard. Mater.* (1991) **28,** 295–311.

4.  Abriola, L.M., Dekker, T.J., and Pennell, K.D.: "Surfactant-Enhanced Solubilization of Residual Dodecane in Soil Columns," *Environ. Sci. Technol.* (1993) **27,** No. 12, 2341–50.

5.  Sabatini, D.A., Knox, R.C., and Harwell, J.H.: "Emerging Technologies in Surfactant-Enhanced Subsurface Remediation," *Surfactant-*

*Enhanced Subsurface Remediation,* D.A. Sabatini, R.C. Knox, and J.H. Harwell (ed.), American Chemical Society, Washington, DC (1995) 1–5.

6. Pope, G.A., and Wade, W.H.: "Lessons from Enhanced Oil Recovery Research for Surfactant-Enhanced Aquifer Remediation," *Surfactant-Enhanced Subsurface Remediation,* D.A. Sabatini, R.C. Knox, and J.H. Harwell (ed.), American Chemical Society, Washington, DC (1995) 142–159.

7. Fountain, J.C., Waddel-Sheets, C., Lagowski, A., Taylor, C., Frazier, D., and Byrne, M.: "Enhanced Removal of Dense Nonaqueous Phase Liquids Using Surfactants," *Surfactant-Enhanced Subsurface Remediation,* D.A. Sabatini, R.C. Knox, and J.H. Harwell (ed.), American Chemical Society, Washington, DC (1995) 178–189.

8. Lake, L.W.: *Enhanced Oil Recovery,* Prentice Hall, Englewood Cliffs, NJ (1989).

9. Abriola, L.M., Pennell, K.D., Pope, G.A., Dekker, T.J., and Luning-Prak, D.J.: "Impact of Surfactant Flushing on the Solubilization and Mobilization of Dense Nonaqueous-Phase Liquids," *Surfactant-Enhanced Subsurface Remediation,* D.A. Sabatini, R.C. Knox, and J.H.

Harwell (ed.), American Chemical Society, Washington, DC (1995) 11–21.

10. Paul, G.W., Lake, L.W., and Pope, G.A.: "A Simplified Predictive Model for Micellar-Polymer Flooding," paper SPE 10733 presented at the 1982 California Regional Meeting of the Society of Petroleum Engineers, San Francisco, CA, March 24–26.

11. Brown, C.L., Pope, G.A., Abriola, L.M., and Sepehrnoori, K.: "Simulation of Surfactant-Enhanced Aquifer Remediation," *Water Resour. Res.* (1994) **30,** No. 11, 2959–77.

12. Datta-Gupta, A., Pope, G.A., Sepehrnoori, K., and Thrasher, R.L.: "A Symetric, Positive Definite Formulation of a Three Dimensional Micellar/Polymer Simulator," *SPE Reservoir Eng.* (1986) **1,** No. 6, 622–632.

13. Delshad, M., Pope, G.A., and Sepehrnoori, K.: "A Compositional Simulator for Modeling Surfactant Enhanced Aquifer Remediation," *J. Contam. Hydrol.* (accepted April 1995).

14. Intera Inc.: *Application of the UTCHEM Simulator to DNAPL Site Characterization and Remediation,* Intera Inc., Austin, TX (Dec. 1994).

15. Datta-Gupta, A. and King, M.J.: "A Semianalytic Approach to Tracer Flow Modeling in Heterogeneous Permeable Media," *Adv. Water Resour.* (1995) **18**, 9–24.

16. Pope, G.A.: "The Application of Fractional Flow Theory to Enhanced Oil Recovery," *SPEJ* (June 1980) 191–205.

17. Deutsch, C.V.: *GSLIB: Geostatistical Software Library and User's Guide,* Oxford University Press, New York (1992).

18. Larson, R.G. and Hirasaki, G.J.: "Analysis of the Physical Mechanisms in Surfactant Flooding," *SPEJ* (Feb. 1978) 42–58.

19. Bear, J.: *Dynamics of Fluids in Porous Media,* Dover Publications, New York (1988).

20. Datta-Gupta, A., Lake, L.L., and Pope, G.A.: "Characterizing Heterogeneous Permeable Media with Spatial Statistics and Tracer Data Using Sequential Simulated Annealing," *Math. Geol.* (1995) **27**, No. 6, 763–787.

21. Larson, R.G.: "The Influence of Phase Behavior on Surfactant Flooding," *SPEJ* (Dec. 1979) 411–422.

# VITA

Name:           Douglas Irvin Tunison

Born:            3 February 1961

Address:       C/O Ellis Ades
PO Box 266
Leon, KS 67074-0266
Ph.: (316) 745-3613

Education:    University of Kansas
B.S., Engineering Physics, 1983

Professional:  Lieutenant, Civil Engineer Corps, United States Navy